Denitrification by bradyrhizobia under feast and famine and the role of the bc1 complex in securing electrons for N_2O reduction

Yuan Gao, Magnus Øverlie Arntzen, Morten Kjos, Lars R. Bakken and Åsa Frostegård

Faculty of Chemistry, Biotechnology and Food Sciences, Norwegian University of Life Sciences, N-1432 Ås, Norway

Abstract

Rhizobia living as microsymbionts inside nodules have stable access to carbon substrates, but also have to survive as free-living bacteria in soil where they are starved for carbon and energy most of the time. Many rhizobia can denitrify, thus switch to anaerobic respiration under low O_2 tension using N-oxides as electron acceptors. The cellular machinery regulating this transition is relatively well-known from studies under optimal laboratory conditions, while little is known about this regulation in starved organisms. It is, for example, not known if the strong preference for N_2O- over NO_3^--reduction in bradyrhizobia is retained under carbon limitation. Here we show that starved cultures of a *Bradyrhizobium* strain with respiration rates 1-18% of well-fed cultures, reduced all available N_2O before touching provided NO_3^-. These organisms, which carry out complete denitrification, have the periplasmic nitrate reductase NapA but lack the membrane-bound nitrate reductase NarG. Proteomics showed similar levels of NapA and NosZ (N_2O reductase), excluding that the lack of NO_3^- reduction was due to low NapA abundance. Instead, this points to a metabolic-level phenomenon where the *bc1* complex, which channels electrons to NosZ via cytochromes, is a much stronger competitor for electrons from the quinol pool than the NapC enzyme, which provides electrons to NapA via NapB. The results contrast the general

notion that NosZ activity diminishes under carbon limitation and suggest that bradyrhizobia carrying NosZ can act as strong sinks for N_2O under natural conditions, implying that this criterion should be considered in the development of biofertilizers.

Importance

Legume cropped farmlands account for substantial N_2O emissions globally. Legumes are commonly inoculated with N_2-fixing bacteria, rhizobia, to improve crop yields. Rhizobia belonging to *Bradyrhizobium*, the micro-symbionts of several economically important legumes, are generally capable of denitrification but many lack genes encoding N_2O reductase and will be N_2O sources. Bradyrhizobia with complete denitrification will instead act as sinks since N_2O-reduction efficiently competes for electrons over nitrate reduction in these organisms. This phenomenon has only been demonstrated under optimal conditions and it is not known how carbon substrate limitation, which is the common situation in most soils, affects the denitrification phenotype. Here we demonstrate that bradyrhizobia retain their strong preference for N_2O under carbon starvation. The findings add basic knowledge about mechanisms controlling denitrification and support the potential for developing novel methods for greenhouse gas mitigation based on legume inoculants with the dual capacity to optimize N_2-fixation and minimize N_2O emission.

Introduction

Bacteria in most natural and engineered environments are faced with fluctuating availability of nutrients and need to adapt to a “feast and famine” lifestyle. While many soil types are rich in total organic carbon, the concentration of bioavailable carbon substrate is low, particularly in

46 non-rhizosphere soil where lack of substrate is a major factor limiting the growth of heterotrophic
47 bacteria (1). It is likely that bacteria in soil are starved most of the time (2) and only experience
48 infrequent episodes of ample provision of carbon substrate, for example as exudates from a root
49 or organic material released during decay of dead (micro)organisms. Bacteria have developed
50 several strategies to survive extended periods of starvation, such as the development of high-
51 affinity uptake systems to scavenge alternative carbon sources from the surroundings, as well as
52 changes in cell morphology, condensation of the nucleoid and decreased protein synthesis to
53 adapt to a low metabolic activity (3). Many bacteria produce carbon-rich storage materials such
54 as PHA (poly-3-hydroxyalkanoates) and glycogen during periods of substrate availability, which
55 can be utilized to sustain a minimum of metabolic activity when deprived of carbon and energy
56 (4,5).

57 Denitrification is the reduction of NO_3^- to N_2 through anaerobic respiration, where the N-
58 oxides are used as terminal electron acceptors when O_2 becomes scarce. This process can be
59 performed by a diverse range of heterotrophic bacteria, archaea and fungi, which use various
60 forms of organic compounds as electron donors to obtain energy (6) or, in some cases, H_2 (7).
61 The last step of denitrification is the reduction of N_2O, a strong climate gas, to harmless N_2,
62 catalyzed by the N_2O reductase (Nos) (8,9). It is found in a diverse range of prokaryotic organisms
63 but has not been reported in eukaryotes. Some denitrifying prokaryotes can perform all steps of
64 denitrification, others only some, and lack of the last step is common due to absence of the *nosZ*
65 gene coding for NosZ , or lack of other essential gene(s) in the *nos* operon (10,11), but the
66 amounts of N_2O released from denitrification in relation to N_2 (the N_2O/N_2 product ratio) is also
67 influenced by transcriptional and post-transcriptional control mechanisms and by various

environmental factors (6,12-19). Denitrification in agricultural soils is a major source of N_2O, accounting for more than 60% of the global anthropogenic emissions (20,21). A steady increase in atmospheric N_2O has been recorded since the start of industrialization, largely driven by increasing and excessive use of synthetic fertilizers (22,23) and these emissions are predicted to continue to increase unless novel mitigation options are developed (24,25).

Although the addition of reactive nitrogen compounds via synthetic fertilizers accounts for the main part of the N_2O emissions from agricultural soil, the N_2O emitted from legume cropped fields is far from negligible. A compilation of data from ca 70 legume cropped fields estimated ca 1.29 kg N_2O-N ha^{-1} during one growing season, while the corresponding data for N-fertilized crops and pastures showed emissions of 3.22 kg N_2O-N ha^{-1} (26). Legumes do not have to rely on uptake of reactive N such as NH_4^+ or NO_3^- but can acquire N through their symbiotic relationship with some groups of bacteria, collectively called rhizobia, which elicit the production of root nodules on the plant inside which the N_2 fixation takes place. In this process, the rhizobia reduce N_2 to NH_3, which the plant cells reduce to glutamine and use to produce amino acids and eventually proteins (27). When this N-rich plant material is degraded, organic N is released and mineralized to NH_3/NH_4^+ which will be oxidized to NO_3^- by nitrifying organisms. The O_2 consumption by the nitrifiers, together with the production of NO_3^- and the availability of organic compounds from the degraded plants, creates conditions that are conducive to denitrification, likely leading to increased N_2O production.

A novel approach to minimize N_2O emissions from agricultural soil is to enhance the populations of N_2O reducing bacteria (25). In the case of legume crops, which are often inoculated with rhizobia to optimize the N_2-fixation, there are a few promising studies reporting

decreased N_2O emissions from soybean fields inoculated with rhizobia with the dual capability of efficient N_2 fixation and N_2O reduction (28,29). Consequently, selection of rhizobial strains for development of commercial inoculants should, ideally, take both these aspects into account. One problem is, however, that far from all rhizobia carry the *nosZ* gene that encodes Nos. There are relatively few surveys of denitrification genes in different groups of rhizobia. Complete denitrification, which includes all four reduction steps of NO_3^- to N_2, has so far mainly been reported for the genus *Bradyrhizobium*, which is the microsymbiont of a range of economically important legume crops such as soybean, cow pea and peanut (30,31). A full set of denitrification reductases in bradyrhizobia include, with few exceptions, the periplasmic NO_3^- reductase NapA; the Cu-containing NO_2^- reductase NirK, the *bc*-type NO reductase cNor and a NosZ belonging to clade I (19,32). We recently investigated the denitrification capacity of bradyrhizobia from two strain collections, one obtained from nodules of legume trees and herbs growing in Ethiopia, the other mainly consisting of strains isolated from nodules of peanut growing in China (18,19). In these collections, 50 and 37% of the isolates, respectively, were complete denitrifiers, while the others generally lacked NosZ and thus were potential N_2O sources. Common to all strains with complete denitrification was a strong preference for N_2O- over NO_3^- reduction. Transcription analysis and proteomics showed comparable expression levels of NapA and NosZ, suggesting a control mechanism at the metabolic level based on competition for electrons between the electron pathways to NosZ and NapC, which the pathway to NosZ apparently wins. This supports the hypothesis proposed by Mania et al. (18): Electrons to both pathways are delivered from the TCA cycle via NADH dehydrogenase to the quinone/quinol pool and channeled either to NapC, which delivers electrons to NapA (via the enzyme NapB), or to the *bc1* complex. Cytochromes will

receive electrons from the *bc1* complex and deliver them to NosZ, and also to nitrite reductase (NirK or NirS depending on the organism) and nitric oxide reductase Nor (cNor or qNor). The competition for electrons between the pathways to NapA and NosZ most likely takes place at the first branching point where the membrane bound *bc1* complex competes very efficiently with the membrane bound NapC for the electrons.

The results presented by Mania et al. and Gao et al. (18,19) were based on experiments with organisms provided with ample amounts of C substrate (electron donor), which is likely to reflect the situation in legume nodules where the microsymbiont receives C from the plant. It can, however, be expected that rhizobia, which may survive for many years in soil (33), spend a large part of their life cycle as free-living organisms in soil where they will experience lack of available C substrate most of the time (2). Rhizobial inoculants that carry NosZ are thus potentially important sinks for N_2O produced both by themselves and by other soil microbes. It is, however, not known if the competition for electrons favoring N_2O reduction in well-fed cultures is retained during substrate limitation ("starvation"). Here we exposed cultures of *Bradyrhizobium* strain HAMBI 2125, also studied in (19), to shorter and extended periods of starvation and analyzed the denitrification kinetics, including the electron flow rates to the individual denitrification reductases. We also quantified the cellular abundancies of Nap, Nir and Nos. The results have practical implications, supporting that these organisms can act as sinks for N_2O under natural conditions. Moreover, the results are ecologically interesting since they show that cultures exposed to extended starvation divided into two opposite denitrification phenotypes, one with very slow metabolism, the other with retained metabolism, possibly reflecting a strategy to increase the chances for survival during periods of starvation.

Results

Denitrification kinetics in cultures prepared following Bioassay 1. Two bioassays were developed for starvation experiments, Bioassay 1 and 2 (Figs. 1A and B). In a first experiment, following Bioassay 1, the denitrification gas kinetics, concentrations of NO_3^- and NO_2^- and electron flow rates to the different reductases were compared for well-fed *vs* starved cultures (Figs. 2A-D). In this bioassay the cultures were allowed to synthesize the denitrification reductases in the presence of ample amounts of substrate. Cultures were raised under fully oxic conditions in YMB medium. When OD_{600} reached 0.1 the headspace was replaced with He. Then, 1% O_2 was injected, corresponding to an initial concentration of 10 µM in the liquid, to allow transition to anaerobic respiration in response to a gradual depletion of O_2. After centrifugation/washing, pellets were pooled and inoculated into flasks containing YMB (9.9E+08 cells $flask^{-1}$) or buffer (5.0E+09 cells $flask^{-1}$), supplemented with 1 mM KNO_3 and 0.25 mM KNO_2, and with He plus 1 ml N_2O (around 80 µmol N) in headspace. The initial O_2 concentration in these flasks was 0.5 µM for cultures with YMB and 0.2 µM in cultures with buffer.

The O_2 was depleted within the first 5 h in both treatments (insets in Figs. 2A and B). The provided NO_2^- and N_2O were reduced simultaneously from the beginning of the incubation in both treatments. The NO_3^- was left untouched in the well-fed cultures until the exogenous N_2O was reduced (Fig. 2A), also seen from lack of electron flow to Nap except for a small peak in electron flow early in the anoxic incubation (Fig. 2C). No NO_3^- reduction took place in the starved cultures throughout the entire incubation period, as seen from the lack of electron flow to Nap (Fig. 2D). The negative V_{eNap} estimated for the starved cultures (inset in Fig. 2D) and the initial

156 phase of the well-fed cultures are probably due to minor errors in calibration of N-gas
157 measurements as well as in parameters used to calculate rates of N-transformation (sampling
158 loss and N_2-leakage, see Molstad et al. (34)), which amounts to substantial errors in the estimates
159 of NO_3^-reduction rates because they are based on N-mass balance (explained in detail by Lim et
160 al. (35)). This implies a relatively high detection limit for NO_3^- reduction, and the negative values
161 cannot be taken as evidence for the complete absence of any electron flow to NO_3^-. However,
162 the measured NO concentrations lend some support to the claim that V_{eNap} was ~0 until depletion
163 of the externally provided N_2O. In the well-fed culture, the concentration of NO declined to zero
164 in response to depletion of NO_2^-, and increased soon after, as V_{eNap} increased (Figs. 2A and C).
165 Likewise, the NO concentration declined to very low values in response to depletion of NO_2^- in
166 the starved culture (Fig. 2B).

167 Fig. 2C and D show the calculated electron flow rates per cell to the individual reductases, and
168 their sum, illustrating their competition for electrons. This shows that the well-fed cells (Fig. 2C)
169 sustained a nearly constant total electron flow rate around 9 fmol e^- $cell^{-1}$ h^{-1} throughout, but
170 allocated to different reductases depending on the availability of electron acceptors: As long as
171 NO_2^- and N_2O were both present, Nos captured around 50% of the electrons ($V_{eNos} \sim V_{eNir} + V_{eNor}$),
172 increasing to 100% when NO_2^- was depleted after 6-7 hours, while the electron flow rate to Nap
173 remained insignificant until the externally provided N_2O became depleted. The starving cells (Fig.
174 2D) had an order of magnitude lower total electron flow rate per cell, declining gradually
175 throughout the incubation, and here Nos captured >> 50% of the electrons during the first 10 h
176 ($V_{eNos} >> V_{eNir} + V_{eNor}$), but declined to ~50% towards the end.

A second experiment was set up according to Bioassay 1 to determine if the individual denitrification reductases were functional during starvation if the appropriate N-oxide was present. The cultures were incubated anoxically ([O_2] <0.21 ±0.04 µM) in C-free buffer, similar to the first experiment, with the difference that only one of the N-oxides (NO_3^-, NO_2^- or N_2O) as initial electron acceptor (Figs. 3A-C). This experiment established that starved cultures readily reduced NO_3^- from the start when no other N-oxide was provided (Fig. 3A). It also demonstrated that the cell specific electron flow to N-oxides was practically unaffected by the type of electron acceptor provided, except for the slightly lower rates initially for flasks with NO_2^-. For all treatments, the cell specific electron flow rate decreased gradually throughout, and the levels are very similar to those observed in the first experiment (Fig. 3D).

Cell size and PHA accumulation of starved vs well-fed cultures. The morphologies of single bacterial cells from different treatments (starved/well-fed and anoxic/oxic) were analyzed by phase contrast microscopy (Fig. S1A). By quantifying cell dimensions, we found marginal but statistically significant effects (Mann-Whitney test, $p < 0.01$) of starvation: while there was no significant difference in cell area of individual cells (Fig. S1B), starved cells were on average ~12% longer and ~5% thinner than well-fed cells (Fig. S1B). By further calculating cell volumes, a slight reduction in average cell volume was observed upon starvation of aerobic cells ($p=0.057$), but not for cells grown under anoxic conditions (Fig. S1C). Furthermore, a qualitative analysis of the presence of PHA granules was done by staining the cells with Nile Red, a lipophilic dye with high affinity for PHA (36). Large foci corresponding to PHA granules were seen in all conditions. It should be noted that, as a lipophilic dye, Nile Red will also bind non-specifically to lipids and

membrane, and based on the imaging performed here, it could not be concluded whether there were any significant differences in PHA content between the conditions.

Denitrification kinetics after providing starving cultures with an artificial electron donor. A third incubation experiment was performed based on Bioassay 1, but TMPD (N, N, N´, N´-tetramethyl-p-phenylenediamine) and ascorbate were added to starved cultures (100 µM and 10 mM, respectively, in the culture medium) to provide cytochrome *c* with an excess of electrons (37,38). Since cultures treated according to Bioassay 1 were able to provide electrons for denitrification (10-18% of the electron flow in well-fed cells during the first 5 h, then decreasing to ca 4%; Fig. 2D), we expected that the TMPD treatment would reduce or eliminate the oxidation of quinol by the *bc1* complex and that this would allow electrons to flow to Nap via NapC, resulting in NO_3^- reduction. We also expected that loading cytochrome *c* with electrons would relieve or weaken the competition for electrons between Nir, Nor and NosZ. The results (Fig. 4) lend little support to the former since the electron flow to Nap remained insignificant until N_2O had been depleted. But the results confirm an effect of TMPD on the competition between Nos and Nir: V_{eNir}, V_{eNor} and V_{eNos} were similar and high (4-5 fmol e^- $cell^{-1}$ h^{-1}) until NO_2^- was depleted. Thus, Nir and Nos competed equally well when the cytochrome *c* pool was fully reduced by TMPD. After depletion of NO_2^-, V_{eNos} leaped to its maximum level, 13-14 fmol N $cell^{-1}$ h^{-1}, and kept this rate until all the exogenous N_2O was depleted.

Denitrification kinetics and reductase abundancies of cultures exposed to extended starvation following Bioassay 2. While Bioassay 1 successfully induced starvation in terms of a

downshift in respiration, the rates did not reach a stable level during the assay but declined gradually throughout, apparently approaching more stable low levels after 20 h. On this background, we introduced a more severe starvation assay (Bioassay 2, Fig. 1B) by including a 20 h aerobic incubation in buffer prior to the starvation-denitrification assay, in order to reach a lower and more stable rate of respiration than in the first experiment. In addition, Bioassay 2 was designed to force the cells to synthesize the denitrification proteome while starving. In several preliminary experiments with Bioassay 2 (results not shown), we found a conspicuous variability between flasks regarding the cell specific respiration rate where one or two out of three replicate flasks had four to six times higher cell respiration rates than the other(s). At first, we suspected that it could be due to impurities of flasks or magnets, but meticulous acid washing failed to remove the stochastic variation. Being convinced that the stochasticity reflects a real regulatory switch of the cultures, we performed a final experiment in which 15 replicate flasks were monitored for denitrification kinetics (Fig. 5).

The cultures received initially 1 mM NO_3^- in the buffer (but no NO_2^-), and He plus 1 ml N_2O (80 µmol N) in headspace. The O_2 concentration at the time of inoculation was <0.5 µM in the liquid. The flasks separated into two distinct denitrification phenotypes (Figs. 5A and B). Nine flasks showed "low" cell specific respiration rates (total electron flow maximum 0.27 fmol e^- $cell^{-1}$ h^{-1}), corresponding to approximately 2.7% compared to well-fed cultures (Fig. 5A), while the other six showed a "fast" respiration rate (total electron flow 1.0-1.8 fmol e^- $cell^{-1}$ h^{-1}). Both phenotypes reduced N_2O from the beginning of the incubation, showing a strong preference for N_2O over NO_3^-. In the flasks with fast respiration, the cells started to reduce NO_3^- in response to

depletion of the externally provided N_2O. In the flasks with slow respiration, N_2O was not depleted within the time frame of the experiment, and NO_3^- reduction remained negligible.

To investigate if cell lysis, and thus release of available C, could explain why some cultures showed the "fast" growth phenotype, we compared the OD_{600} and the number of viable cells in "slow" *vs* "fast" cultures. The samples were taken after incubation for 3.1 h in anoxic buffer, when the two phenotypes were clearly distinct (Fig. S2A) but when some possible growth of cells in the "fast" cultures would not yet hide if lysis had occurred. The OD_{600} spanned from 0.12-0.13 with no statistical difference ($p>0.3$) between cultures with "fast" and "slow" respiration. Similarly, no difference ($p=0.4$) was found for the viable counts which showed 1.21E+10 to 1.33E+10 CFU $flask^{-1}$ for the "fast" cultures and 1.23E+10 to 1.34E+10 CFU $flask^{-1}$ for the "slow" cultures (Fig. S2B).

We also tested the metabolic integrity of the cells in the flasks with slow respiration by injecting C-substrates (YMB) to the flasks after 24.8 hours, which proved their capacity to quickly regain activity approaching that of well-fed cells (Fig. 5A). A close inspection of the cell specific electron flow rate showed an immediate increase in V_{eNos}. To investigate if the observed divergencies in phenotypes were due to differences in denitrification reductase abundancies, we quantified the relative abundances of Nap, NirK and NosZ in samples taken at different time points throughout the incubations (Figs. 5E and F), together with the corresponding denitrification kinetics (Figs. 5A and B) and cell specific electron flow to reductases (Figs. 5C and D). The membrane-bound NO reductase (cNor) could not be extracted quantitatively (the results showed 1000 times lower abundancies than for the other denitrification reductases) and is therefore not shown. The inoculum had been cultured aerobically for 3-4 generations, never permitting the OD_{600} to exceed 0.1, to ensure that any denitrification enzymes would be diluted

to extinction by aerobic growth, assuming that the transcription of all genes is effectively repressed by oxygen. This strategy was apparently successful since Nap and Nir were undetectable at the start of the anoxic incubation. NosZ, on the other hand, was detected also in the aerobic cultures, suggesting that the *nosZ* gene is constitutively transcribed at low levels in these organisms.

After transferring the cells to anoxic buffer, the abundance of all three reductases increased both in cultures with "slow" and "fast" respiration. Cultures with "slow" respiration rate synthesized less denitrification reductases than those with "fast" respiration rate during the first 20 h. The relative abundances of the different reductases also differed between the two phenotypes. In cultures with "slow" respiration, NosZ was significantly more abundant than Nap and Nir ($p<0.01$), which were comparable (Fig. 5E). Cultures with "fast" respiration instead contained higher abundancies of NosZ and Nir compared to Nap at 5 h. After this, the abundance of Nir increased more than that of the others and at 20 h the LFQ of Nir was 0.20 ± 0.07, while the abundancies of NosZ and Nap were approximately half of that (Fig. 5F). After addition of carbon substrate to the cultures with "slow" respiration, a rapid synthesis of all three reductases took place. This synthesis was most prominent for Nir which, after a couple of hours, had increased three-fold, reaching a relative abundance that was twice as high as Nap and NosZ (Fig. 5E), resembling the abundance profile of the cultures with "fast" respiration (Fig. 5F).

Discussion

Detailed eco-physiological studies during the past decades have revealed several aspects of how the denitrification process is regulated in different organisms (6,13,39). Most of this

knowledge is, however, based on laboratory studies where cultures have been grown under optimal conditions, while less attention has been paid to understanding how denitrification, and particularly the release of N_2O, is affected if cells are starved, which is the normal state of cells in most natural environments. We focused on how starvation, i. e. lack of carbon substrate, affects denitrification and N_2O release. The general notion has been that N_2O reductase is less competitive for electrons than the other denitrification reductases, leading to emissions of N_2O when the availability of electron donors is low. This is largely based on a single study of *Alcaligenes faecalis* (40) and has been supported by some studies of complex communities but contested by others (41-43). *A. faecalis* can perform partial denitrification reducing NO_2^- to N_2 using NirK, cNor and NosZ clade I, but this organism lacks dissimilatory NO_3^- reductases (Nar or Nap). The study by Schalk-Otto (40), performed in continuous cultures, showed increased N_2O release under low substrate concentrations, and it was suggested that N_2O reductase did not compete successfully with the other reductases for electrons from cytochrome *c*, possibly due to lower affinity for the electron donor. This conclusion needs, however, further verification by more detailed studies of the mechanism involved. Moreover, such studies need to be extended to other groups of denitrifying microorganisms and should include organisms carrying a complete denitrification pathway (thus with Nar and/or Nap). Research over the past decades has revealed diverse denitrification phenotypes among even closely related bacteria, with implications for their accumulation of denitrification intermediate products (15,44).

The denitrification phenotype described for a range of taxonomically diverse *Bradyrhizobium* strains with a complete denitrification pathway is characterized by a strong preference for N_2O over $NO_3^-$when grown in full-strength YMB medium under denitrifying conditions (18,19). The

present study provides compelling evidence that this preference is retained when the organisms are starved for carbon and energy, with practically no electron flow to Nap when N_2O was present (Figs. 2A-D). It seems unlikely that this would be due to too low levels of Nap, both because the cultures showed well-functioning Nap activity if NO_3^- was provided as the only initial electron acceptor (Fig. 3A) and because the cultures were able to produce comparable amounts of Nap, Nir and Nos even when grown under severe starvation conditions using Bioassay 2 (Proteomics results, Figs. 5E and F). Therefore, the lack of NO_3^- reduction during the period when there was N_2O in the system could not be explained by a lack of Nap molecules. Instead, the results suggest the same metabolic-level phenomenon as found for well-fed cultures in this study (Fig. 2A) and earlier (18,19), where NosZ outcompetes Nap for electrons, leaving Nap virtually without electrons so long as exogenous N_2O is available. In theory, the observed lack of NO_3^- reduction in the presence of N_2O could be due to a direct inhibition of NapA by N_2O, but this is refuted by the results of Mania et al. (18), who observed high NapA activity in cells exposed to 10 vol% N_2O, when NosZ was inhibited by acetylene (Table 2 in (18)). These results are analyzed and discussed in more detail Fig. S3.

The attempt to tweak the electron flow toward Nap by the addition of TMPD and ascorbate did not result in measurable NO_3^- reduction in the starved cultures (Fig. 4A). A recent study by Mania et al. (18) demonstrated that well-fed *Bradyrhizobium* cells did reduce some NO_3^- in the presence of N_2O, if provided with TMPD and ascorbate. This suggested that a cytochrome *c* pool that was strongly reduced by TMPD allowed Nap to receive a minimum of the electrons from quinol, delivered from the TCA cycle. The specificity of the electron delivery from TMPD to cytochrome *c* cannot be taken for granted, however, and the result by Mania et al. (18) could

instead reflect a minimum of electron flow from TMPD to quinone or to NapC, directly, or indirectly. In the present experiment with starved cells, TMPD + ascorbate failed to induce measurable electron flow to Nap in the presence of N_2O (Fig. 4B). The contrasting results for well-fed *versus* starved cells probably reflects the marginal electron flow from the TCA cycle to the quinone/quinol pool in the starved cells. A separate experiment supported this, showing that when carbon substrate (YMB) was added to starved cultures, this provided enough electrons to support some Nap activity, although NosZ activity still dominated (Fig. S4).

At the same time, the result refutes the concerns regarding unspecific electron delivery of electrons from TMPD to quinone. Functional Nap was apparently present, and NO_3^- reduction started when N_2O was almost depleted, with V_{eNap} being 2 fmol e^- $cell^{-1}$ h^{-1} which was twice as high as $V_{eNir/Nor}$ (Fig. 4B). The latter is as expected, since the reduction of 1 mole of NO_3^- to NO_2^- requires 2 mole electrons, while reduction of NO_2^- and NO requires 1 mole electrons. Furthermore, the electron flow to NosZ was the same as to Nir and Nor, suggesting that Nir and NosZ competed equally well for electrons from cytochrome *c*. The maximum total electron flow of 13-14 fmol e^- $cell^{-1}$ h^{-1} when the cytochrome *c* pool was saturated with electrons from TMPD is likely to be close to the maximum capacity of the denitrification pathway. This electron flow rate is higher than the total electron flow rate in the well-fed cells, which was 8-10 fmol e^- $cell^{-1}$ h^{-1} (Fig. 2C). The factor limiting V_{eNos} to 13-14 fmol $cell^{-1}$ h^{-1} is plausibly the rate of electron delivery from cytochrome *c* and/or k_{cat} for Nos. Of note, Nir and NosZ received equal shares of the electron flow when delivered by TMPD via cytochrome *c* (Fig. 4B), while NosZ clearly outcompeted Nir under normal respiration, when electrons were delivered via quinol (Fig. 2C and D). This contrast

351 indicates that the competitive edge of NosZ versus Nir under normal respiration is due to an
352 alternative electron flow to NosZ via NosR, as suggested previously (18).
353
354 In another experiment we added YMB medium to “slow respiration” phenotypes of the
355 cultures that had been exposed to extended starvation (Figs. 5A, C and E). These cultures had
356 some NosZ activity (V_{eNos} 0.1-0.3 fmol e^- $cell^{-1}$ h^{-1}), while Nap and Nir activities could not be
357 detected. Addition of the electron donor (YMB) led to an immediate upshoot in the activities of
358 all reductases. This could not have been the case if the reductases were not present already,
359 which was proven by the proteomics results. Taken together, the results support that the
360 absolute preference for N_2O over NO_3^- was due to competition for electrons, also under severe
361 starvation conditions.
362 It is well known that bacteria have developed a range of physiological responses to tackle
363 starvation. Some survive by forming spores, but most bacteria survive by strongly reduced
364 metabolic rates and minimizing the synthesis of some proteins while upregulating others such as
365 genes for high-affinity transporters, essential repair mechanisms and alternative energy sources
366 (3,45,46). Some such changes have been observed in rhizobia belonging to *Rhizobium*
367 *leguminosarum*, which stayed viable for long periods (55 days) of C starvation (47). Changes in
368 cell size are common during long-term starvation, sometimes leading to the formation of small
369 or even ultra-microcells which may have increased tolerance to antibiotics and other stresses
370 (2,46). Another way for many bacteria, including rhizobia, to survive is to use carbon stored as
371 polyhydroxyalkanoates (PHA) or glycogen, formed during periods of ample nutrient abundance
372 (48). In the present study, the metabolic activity, measured as anaerobic respiration rate,

decreased to between 1 and 18% that of well-fed cultures, depending on which starvation bioassay was used. We did not, however, detect any obvious decrease in cell size when comparing cells starved for 24 h, although cell morphologies were slightly altered (Figs. S1A and B). PHA was observed in the starved cells as well as well-fed ones, as shown with Nile red staining (Fig. S1A) and no obvious reduction in PHA could be observed during starvation from our assays. Since this was a comparably short period of starvation, it is conceivable that the cells would make use of the stored carbon if the starvation was prolonged. It could be speculated that one reason for not using the PHA reserves (and glycogen) immediately, is that these are saved to be used during bacteroid formation (48). To clarify these issues, more detailed studies are however needed.

A striking separation into two phenotypes during starvation, as shown in Fig. 5, was observed in repeated experiments (Bioassay 2), each time with about two thirds of the flasks showing a "fast" and the others "slow" respiration: 1.0-1.8 fmol e^- $cell^{-1}$ h^{-1} vs 0.1-0.3 fmol e^- $cell^{-1}$ h^{-1}, respectively. Phenotypic heterogeneity has been observed in single-strain cultures of various bacteria when exposed to carbon substrate deficiency and may, or may not, be due to mutations during starvation for one week or more (3,49). Mutations in the entire population in several replicate flasks are unlikely and cannot, however, have caused the rapid diversification into "slow"- or "fast" respiration in the present study. It may instead reflect a stochastic phenomenon, or that the culture contained different subpopulations. We speculated that the "fast respiration" phenotype may be due to a fraction of the cells dying, allowing the other cells to survive on nutrients released from lysed cells, as seen for other bacteria (3). However, this would require lysis of a substantial fraction of the cells, which is refuted by the observation that the flasks with

395 "slow" and "fast" phenotypes had practically identical numbers of viable cells (Fig. S2). Thus,
396 further studies are needed to understand this phenomenon of different respiration rates.
397 Although the starvation bioassays developed for this study cannot be regarded as a close
398 mimicking of the conditions in natural environments, it is conceivable from the experiments that
399 these organisms are potentially strong sinks for N_2O when living in soil under fluctuating
400 availability of carbon substrate. Bioassay 1 is probably closer to a "real-world" situation than
401 Bioassay 2, since it is likely that denitrifying bacteria experience regular fluctuations in oxygen
402 and thus are not devoid of denitrification reductases if they enter starvation. On the other hand,
403 Bioassay 2, where the cells had to produce the denitrification proteome in the absence of
404 external electron donors (C-substrate), showed that even under these conditions N_2O reduction
405 strongly dominated over NO_3^- reduction.
406
407 **Materials and methods**
408 **Bacterial strain and culture preparations.** *Bradyrhizobium* strain HAMBI 2125, originally
409 isolated from nodules of *Arachis hypogaea* growing in Sichuan, China (50), was used in all
410 experiments. This strain, which is closely related to *Bradyrhizobium ottawaense*, contains the
411 genes needed for complete denitrification (19). A culture was raised from one single colony after
412 streaking on agar plates. After checking the purity by sequencing the 16S rRNA gene (19),
413 portions were preserved in 15% glycerol at -80 °C. Cultures for all the experiments were started
414 from the -80 °C stocks and raised under fully oxic conditions in 120 ml serum flasks containing 50
415 ml Yeast Mannitol Broth (YMB): 10 g l^{-1} D-Mannitol, 0.5 g l^{-1} K_2HPO_4, 0.2 g l^{-1} $MgSO_4 \cdot 7H_2O$, 0.1 g
416 l^{-1} NaCl and 0.5 g l^{-1} yeast extract (51). All incubations were done at 28 °C. Medical flasks (120 ml)

were used in all experiments. A magnet in each flask secured vigorous stirring (600-700 rpm) to avoid cell aggregation and to optimize the gas exchange between liquid and gas phases (18). To prevent that the cells experienced anoxia during this oxic incubation, and thus to avoid de novo synthesis of denitrification reductases, portions were regularly transferred to new flasks containing fresh medium, so that the OD_{600} was never allowed to exceed 0.1 (19). These aerobically grown cultures were used as inoculants in the "starvation bioassays" described below.

Flasks for denitrification experiments were prepared as described in (18). Briefly, flasks (120 ml) containing 50 ml buffer (or medium) were capped with sterilized, gas tight butyl rubber septa (Matrix AS, Norway). The air was removed by applying vacuum repeatedly (6 x 360 s) and He was then filled for 30 s, after which the overpressure was released. The flasks were left for two days to equilibrate the gases between the headspace and liquid (52). Before starting the experiment, 0.7 ml or 1 ml O_2 (equal to 1 or 1.5 vol %) and 1 ml N_2O (70 to ~80 µmol N $flask^{-1}$) was injected into the headspace and sterile filtered solutions of KNO_3 (and sometimes KNO_2) were added to the liquid reaching initial, desired concentrations (0.25 -1 mM).

Starvation bioassays. Starvation bioassays were established, which followed one of the procedures described in Fig. 1. In Bioassay 1 "Mild starvation", cultures were allowed to make the transition to denitrification in full-strength YMB before being exposed to starvation. Oxically grown, well-fed cultures were incubated for 48 h after which the headspace was replaced by He and 1% O_2, and 1 mM KNO_3 was added to the medium. When O_2 was depleted, the cultures were centrifuged (10 000 × g at 4 °C for 10 min) and washed twice in sterile ddH_2O. The pellets (triplicates) were pooled to reduce bias in the form of variations due to the

centrifugation/washing. Each pellet was divided into three and used to inoculate flasks containing 50 ml C-free buffer supplemented with 1 mM KNO_3 and 0.25 or 0.5 mM KNO_2. These flasks had been made anoxic (O_2 <0.5 µM in the liquid) and contained He and/or 1 ml N_2O (around 80 µmol N $flask^{-1}$) in the headspace. When incubated in the buffer, the respiration rate of the cultures was 10-18% that of well-fed cultures during the first 15 h, then it decreased to about 4%.

In Bioassay 2 ("extended starvation"), denitrification was instead induced after having exposed the cells to starvation for 20 h. The cultures were raised in fully oxic flasks containing YMB medium. When OD_{600} reached ~0.1, the cultures were centrifuged (10 000 × g at 4 °C for 10 mins) and washed twice in sterile ddH_2O. The pellets (triplicates) were pooled after which they were evenly divided and used to inoculate fully oxic flask containing C-free "starvation buffer". These cultures were incubated for 20 h, then centrifuged after which the pellets were pooled and divided evenly before being inoculated into flasks containing C-free "starvation buffer" with 1 mM KNO_3, and with He and 1 ml N_2O (around 80 µmol N $flask^{-1}$) in headspace. These flasks had been made anoxic (O_2 <0.5 µM in the liquid). The respiration rate of cultures exposed to "extended starvation" was ca 1-4% compared to that of well-fed cultures. Results from the different starvation bioassays were compared to those from well-fed cultures. To avoid biases, the treatments, which were in all cases set up at least in triplicates ($n \geq 3$), were the same regarding centrifugations and washings until the last step when pooled cells were inoculated to anoxic flasks containing either YMB or buffer. The carbon source in the YMB medium comprised >200 times surplus of electron donor compared to electron acceptors throughout all incubations, thus ensuring that the electron donor was not depleted. All cultures were incubated at 28°C, and with vigorous stirring (600-700 rpm).

Addition of YMB medium or TMPD as electron donors to starved cultures. Experiments were performed to investigate how starved cultures of *Bradyrhizobium* strain HAMBI 2125 responded to the addition of an electron donor, either provided as an artificial electron donor (Fig. 4) or as YMB medium (2 ml mannitol /yeast solution providing them with a substrate concentration corresponding to half-strength YMB, thus 5 g mannitol and 0.25 g yeast l^{-1}, Fig. 5). As artificial electron donor we used sodium TMPD (N, N, N´, N´-tetramethyl-p-phenylenediamine) which, in the presence of ascorbate, donates electrons to cytochrome c thus providing electrons to Nir and NosZ (18,37). Ascorbate and TMPD (both from Sigma-Aldrich®, Germany) were dissolved in ddH_2O or 96% ethanol, respectively, and filter sterilized. The solutions were added to the incubation flasks 10-15 mins before gas sampling. The effect of different concentrations of TMPD (100, 250, and 500 µM in the culture buffer) combined with 10 mM ascorbate on N_2O reduction was checked prior to the main experiments. This showed that 500 µM TMPD had an obvious inhibition effect on N_2O reduction, while 100 µM and 250 µM showed no inhibitory effect (not shown). To minimize other, possible effects we used 100 µM TMPD for the experiments (as done in Mania et al. (18)). In another experiment, shown in Fig. S4, 4 ml of a mannitol/yeast solution was added to flasks containing 50 ml starved cultures, providing them with a substrate concentration corresponding to full strength YMB (10 g mannitol and 0.5 g yeast l^{-1}).

Monitoring of gas kinetics, NO_3^- and NO_2^- concentrations and electron flow rates. The culture flasks were placed in a robotized incubation system and the headspace gas was sampled frequently for N_2, N_2O, NO and O_2 measurements (34). Gas losses caused by sampling were taken

into account when calculating the production and consumption of gases, as described by Molstad et al. (34) and Mania et al. (18). The concentration of O_2 in the anoxic incubation flasks was <0.6 µM at the start of the experiment, which was well below the level for initiating denitrification (4.6 µM; (19)).

The NO_2^- concentrations were monitored as described in Mania et al. (18). Briefly, samples (0.1- 0.5 ml) were taken every 1 or 2 hours (n=3) from the liquid phase through the septum of the flasks using a sterile syringe. To avoid that the gas kinetics was affected by the sampling, a set of flasks was dedicated to NO_2^- measurements and a parallel set was left untouched for gas measurements. NO_2^- was determined using a chemoluminescence NOx analyzer (Sievers NOA^{TM} 280i, GE Analytical Instruments) after at first reducing the NO_2^- to NO by adding 10 µl liquid sample into a purging device containing a reducing agent (50% acetic acid with 1% (w/v) NaI) (53,54). The NO_2^- concentrations were determined against a standard curve (range 0-2 mM NO_2^-; r^2= 0.999).

The cell specific electron flow rates (V_e, mol e^- $cell^{-1}$ h^{-1}) for each time increment between two gas samplings were calculated as $V_{eflask}(t)/(N(0)+E_{cum}(t)*Y)$, where $V_{eflask}(t)$ is the electron flow rate in the flask (mol e^- $flask^{-1}$ h^{-1}) calculated from measurements, $N(0)$ is number of cells in the flask at time=0, $E_{cum}(t)$ is the cumulated electron flow (mol e^- $flask^{-1}$) at time=t , and Y is the yield per mol electron (cells mol^{-1} e^-) for HAMBI 2125 as measured previously (19). The conversion factor 5.8E8 cells ml^{-1} *OD_{600}^{-1} was used to convert OD_{600} to cell numbers (19).

Proteomics. The abundances of Nap, Nir and NosZ were quantified in starved cultures treated as described for Bioassay 2 (extended starvation). Altogether eighteen flasks were prepared

505 according to Fig. 1B. After the 20 h aerobic incubation in C-free buffer, three flasks were
506 harvested for proteomics analysis and, following centrifugation/washing, the three cell pellets
507 from these flasks were frozen individually at -20 °C. The cultures in the other flasks were pooled
508 three by three and after centrifugation/washing, each cell pellet was divided in three and used
509 to inoculate new flasks containing C-free buffer with NO_3^- in the liquid and with He and 1 ml N_2O
510 in the headspace (Fig. 1B). These flasks (fifteen in total) were placed in the robotic incubation
511 system for monitoring of gas kinetics and NO_2^- concentrations as described above. The entire
512 culture volume (50 ml) was harvested from each of triplicate flasks at different time points during
513 the anoxic incubation. The cultures in six of the flasks showed a "fast" respiration rate (total
514 electron flow 1.0-1.8 e^- $cell^{-1}$ h^{-1}) and were harvested at 5 and 20 h of incubation in anoxic buffer
515 (triplicates at each sampling point). The cultures in the other nine flasks showed a "slow"
516 respiration rate (maximum total electron flow rate was 0.27 fmol e^- $cell^{-1}$ h^{-1}). Six of them were
517 harvested in triplicates after 10 and 20 h in anoxic buffer. The remaining three flasks from the
518 cultures with "slow" respiration rate received a portion of YMB at 24.8 hand were harvested at
519 27 h. Harvested cell cultures were centrifuged and stored as pellets at -20 °C. The protein
520 extraction was as described in Gao et al. (19). Briefly, the thawed cell pellets were resuspended
521 in lysis buffer (20 mM Tris–HCl pH 8, 0.1% v/v Triton X-100, 200 mM NaCl, 1 mM DTT). They were
522 then subjected to bead beating (3 × 45 s) with glass beads (particle size ≤ 106 µm; Sigma) using a
523 MP Biomedicals™ FastPrep-24™ (Thermo Fischer Scientific) at maximum power and with cooling
524 on ice between the cycles. After centrifugation to remove cell debris (10 000 × g; 5 min), the
525 supernatant, containing water soluble proteins, was used for proteomic analysis using an
526 Orbitrap mass spectrometer (described in (19,55)). Quantification was based on LFQ (label-free

quantification) in MaxQuant (56), and the relative abundance of the individual reductases was calculated as percentages of the sum of all protein abundances for each time point. The nitric oxide reductases NorB/C were not measured since only a small fraction of these membrane-bound enzymes can be accurately obtained with this extraction protocol (approximately 1/1000th the quantity of the other reductases).

Viable counts and microscopy. The number of viable cells in starved cultures showing slow and fast respiration rates, observed in flasks prepared according to Bioassay 2, was determined by plating dilutions of the cultures on yeast-mannitol agar (YMA). The morphology of cells from well-fed cultures and starved cultures was compared using phase contrast microscopy and a qualitative determination (presence/absence) of PHA was done by staining with Nile Red (Sigma-Aldrich) followed by fluorescence microscopy. Microscopy was performed on a Zeiss AxioObserver with an Orca-Flash4.0 CMOS camera (Hamamatsu Photonics) controlled by the ZEN Blue software. Images were taken with a 100x phase contrast objective. A HPX-120 Illuminator was used as light source for fluorescence microscopy. Images were prepared using ImageJ and analysis of cell sizes was done using the ImageJ-plugin MicrobeJ (57).

Data availability

Raw data from gas measurements and microscopy can be made available upon request. The mass spectrometry proteomics data have been deposited to the ProteomeXchange Consortium via the PRIDE (58) partner repository with the dataset identifier PXD038844.

Acknowledgements

This project was supported by Kingenta Ecological Engineering Group Co., LTD and by the project PASUSI financed by the EC Horizon2020 ERA-NET Cofund Programme, Grant agreement No. 727715 and by the Research Council of Norway, projects No. 290488 and 325770. Yuan Gao is grateful to the China Scholarship Council (CSC) for financial support. We thank Gro Stamsås for help with microscopy.

Ethics declarations

The authors declare that they have no conflict of interest.

References

1. Hobbie JE, Hobbie EA. 2013. Microbes in nature are limited by carbon and energy: The starving-survival lifestyle in soil and consequences for estimating microbial rates. Front Microbiol 4:324.
2. Morita RY. 1990. The starvation-survival state of microorganisms in nature and its relationship to the bioavailable energy. Experientia 46:813–817.
3. Bergkessel M, Basta DW, Newman DK. 2016. The physiology of growth arrest: Uniting molecular and environmental microbiology. Nat Rev Microbiol 14:549–562.
4. Ratcliff WC, Kadam SV, and Denison, R.F. 2008. Poly-3-hydroxybutyrate (PHB) supports survival and reproduction in starving rhizobia. FEMS Microbiol Ecol 65:391–399.

5. Müller-Santos M, Koskimäki JJ, Alves LPS, de Souza EM, Jendrossek D, Pirttilä AM. 2021. The protective role of PHB and its degradation products against stress situations in bacteria. FEMS Microbiol Rev 45:fuaa058.
6. Zumft WG. 1997. Cell biology and molecular basis of denitrification. Microbiol Mol Biol Rev 61:533–616.
7. Duffner C, Kublik S, Fösel B, Frostegård Å, Schloter M, Bakken L, Schulz S. 2022. Genotypic and phenotypic characterization of hydrogenotrophic denitrifiers. Environ Microbiol 24:1887-1901.
8. Schneider LK, Wüst A, Pomowski A, Zhang L, Einsle O. 2014. No laughing matter: The unmaking of the greenhouse gas dinitrogen monoxide by nitrous oxide reductase. Met Ions Life Sci 14:177–210.
9. Hein S, Simon J. 2019. Bacterial nitrous oxide respiration: electron transport chains and copper transfer reactions. Adv Microb Physiol 75:137–175.
10. Shapleigh JP. 2013. Denitrifying prokaryotes: Prokaryotic Physiology and Biochemistry. In Rosenberg E, DeLong EF, Lory S, Stackebrandt E, Thompson F. (eds), The prokaryotes, pp. 405-425. Berlin, Heidelberg: Springer.
11. Graf DRH, Jones CM, Hallin S. 2014. Intergenomic comparisons highlight modularity of the denitrification pathway and underpin the importance of community structure for N_2O emissions. PLoS ONE 9:e114118.
12. Richardson D, Felgate H, Watmough N, Thomson A, Baggs E. 2009. Mitigating release of the potent greenhouse gas N_2O from the nitrogen cycle - could enzymic regulation hold the key? Trends Biotechnol 27:388-97.

13. Spiro S. 2012. Nitrous oxide production and consumption: regulation of gene expression by gas-sensitive transcription factors. Philos Trans R Soc Lond B Biol Sci 367:1213-25.
14. Liu B, Frostegård Å, Bakken LR. 2014. Impaired reduction of N_2O to N_2 in acid soils is due to a posttranscriptional interference with the expression of *nosZ*. mBio 5:e01383-14.
15. Liu B, Mao Y, Bergaust L, Bakken LR, Frostegård A. 2013. Strains in the genus *Thauera* exhibit remarkably different denitrification regulatory phenotypes. Environ Microbiol 15:2816-28.
16. Gaimster H, Alston M, Richardson DJ, Gates AJ, Rowley G. 2018. Transcriptional and environmental control of bacterial denitrification and N_2O emissions. FEMS Microbiol Lett 365:1-8.
17. Lycus P, Soriano-Laguna MJ, Kjos M, Richardson DJ, Gates AJ, Milligan DA, Frostegård Å, Bergaust L, Bakken LR. 2018. A bet-hedging strategy for denitrifying bacteria curtails their release of N_2O. Proc Natl Acad Sci 115:11820–11825.
18. Mania D, Woliy K, Degefu T, Frostegård Å. 2020. A common mechanism for efficient N_2O reduction in diverse isolates of nodule-forming bradyrhizobia. Environ Microbiol 22:17–31.
19. Gao Y, Mania D, Mousavi SA, Lycus P, Arntzen M, Woliy K, Lindström K, Shapleigh JP, Bakken LR, Frostegård Å. 2021. Competition for electrons favours N_2O reduction in denitrifying *Bradyrhizobium* isolates. Environ Microbiol 23:2244–2259.
20. Butterbach-Bahl K, Baggs EM, Dannenmann M, Kiese R, Zechmeister-Boltenstern S. 2013. Nitrous oxide emissions from soils: How well do we understand the processes and their controls? Philos Trans R Soc Lond B Biol Sci 368:20130122.

21. Thompson RL, Lassaletta L, Patra PK, Wilson C, Wells KC, Gressent A, Koffi EN, Chipperfield M, Winiwarter W, Davidson EA, Tian H, Canadell JG. 2019. Acceleration of global N_2O emissions seen from two decades of atmospheric inversion. Nat Clim Change 9:993–998.
22. Tian H, Lu C, Ciais P, Michalak AM, Canadell JG, Saikawa E, Huntzinger DN, Gurney KR, Sitch S, Zhang B, Yang J, Bousquet P, Bruhwiler L, Chen G, Dlugokencky E, Friedlingstein P, Melillo J, Pan S, Poulter B, Prinn R, Saunois M, Schwalm CR, Wofsy SC. 2016. The terrestrial biosphere as a net source of greenhouse gases to the atmosphere. Nature 531:225–228.
23. Tian H, Xu R, Canadell JG, Thompson RL, Winiwarter W, Suntharalingam P, Davidson EA, Ciais P, Jackson RB, Janssens-Maenhout G, Prather MJ, Regnier P, Pan N, Pan S, Peters GP, Shi H, Tubiello FN, Zaehle S, Zhou F, Arneth A, Battaglia G, Berthet S, Bopp L, Bouwman AF, Buitenhuis ET, Chang J, Chipperfield MP, Dangal, SRS, Dlugokencky E, Elkins JW, Eyre BD, Fu B, Hall B, Ito A, Joos F, Krummel PB, Landolfi A, Laruelle GG, Lauerwald R, Li W, Lienert S, Maavara T, MacLeod M, Millet DB, Olin S, Patra PK, Prinn RG, Raymond PA, Ruiz DJ, van der Werf GR, Vuichard N, Wang J, Weiss RF, Wells KC, Wilson C, Yang J, Yao Y. 2020. A comprehensive quantification of global nitrous oxide sources and sinks. Nature 586: 248–256.
24. Davidson EA, Kanter D. 2014. Inventories and scenarios of nitrous oxide emissions. Environ Res Lett 9:105012.
25. Bakken LR, Frostegård Å. 2020. Emerging options for mitigating N_2O emissions from food production by manipulating the soil microbiota. Curr Opin Environ Sustain 47:89–94.
26. Jensen ES, Peoples MB, Boddey RM, Gresshoff PM, Henrik HN, Alves BJR, Morrison MJ. 2012. Legumes for mitigation of climate change and the provision of feedstock for biofuels and biorefineries. A review. Agron Sustain Dev 32:329-364.

27. Poole P, Ramachandran V, Terpolilli J. 2018. Rhizobia: From saprophytes to endosymbionts. Nat Rev Microbiol 16:291–303.
28. Hénault C, Revellin C. 2011. Inoculants of leguminous crops for mitigating soil emissions of the greenhouse gas nitrous oxide. Plant Soil 346:289–296.
29. Itakura M, Uchida Y, Akiyama H, Hoshino YT, Shimomura Y, Morimoto S, Tago K, Wang Y, Hayakawa C, Uetake Y, Sánchez C, Eda S, Hayatsu M, Minamisawa K. 2013. Mitigation of nitrous oxide emissions from soils by *Bradyrhizobium japonicum* inoculation. Nat Clim Change 3:208–212.
30. Jaiswal SK, Dakora FD. 2019. Widespread distribution of highly adapted *Bradyrhizobium* species nodulating diverse legumes in Africa. Front Microbiol 10:310.
31. Woliy K, Degefu T, Frostegård Å. 2019. Host Range and Symbiotic Effectiveness of N_2O Reducing Bradyrhizobium Strains. Front Microbiol 10:2746.
32. Bedmar EJ, Robles EF, Delgado MJ. 2005. The complete denitrification pathway of the symbiotic, nitrogen-fixing bacterium *Bradyrhizobium japonicum*. Biochem Soc Trans 33:141-144.
33. Narozna D, Pudełko K, Króliczak J, Golińska B, Sugawara M, Mądrzak CJ, Sadowsky MJ. 2015. Survival and competitiveness of *Bradyrhizobium japonicum* strains 20 years after introduction into field locations in Poland. Appl Environ Microbiol 81:5552–5559.
34. Molstad L, Dörsch P, Bakken LR. 2007. Robotized incubation system for monitoring gases (O_2, NO, N_2O, N_2) in denitrifying cultures. J Microbiol Methods 71:202–211.
35. Lim NYN, Frostegård Å, Bakken LR. 2018. Nitrite kinetics during anoxia: The role of abiotic reactions versus microbial reduction. Soil Biol Biochem 119:203–209.

655 36. Spiekermann P, Rehm BH, Kalscheuer R, Baumeister D, Steinbüchel A. 1999. A sensitive,
656 viable-colony staining method using Nile red for direct screening of bacteria that accumulate
657 polyhydroxyalkanoic acids and other lipid storage compounds. Arch Microbiol 171:73-80.
658 37. Kimelberg HK, Nicholls P. 1969. Kinetic studies on the interaction of TMPD with cytochrome
659 *c* and cytochrome *c* oxidase. Arch Biochem Biophys 133:327–335.
660 38. Bueno E, Richardson DJ, Bedmar EJ, Delgado MJ. 2009. Expression of *Bradyrhizobium*
661 *japonicum* cbb3 terminal oxidase under denitrifying conditions is subjected to redox control.
662 FEMS Microbiol Lett 298:20–28.
663 39. Torres MJ, Simon J, Rowley G, Bedmar EJ, Richardson DJ, Gates AJ, Delgado MJ. 2016. Nitrous
664 Oxide Metabolism in Nitrate-Reducing Bacteria: Physiology and Regulatory Mechanisms. Adv
665 Microb Physiol 68:353-432.
666 40. Schalk-Otte S, Seviour R, Kuenen J, Jetten MSM. 2000. Nitrous oxide (N_2O) production by
667 *Alcaligenes faecalis* during feast and famine regimes. Water Res 34:2080-2088.
668 41. Itokawa H, Hanaki K, Matsuo T. 2001. Nitrous oxide production in high-loading biological
669 nitrogen removal process under low COD/N ratio condition. Water Res 35:657-664.
670 42. Lu H, Chandran K. 2010. Factors promoting emissions of nitrous oxide and nitric oxide from
671 denitrifying sequencing batch reactors operated with methanol and ethanol as electron
672 donors. Biotechnol Bioeng 106:390-8.
673 43. Pan Y, Ni BJ, Bond PL, Ye L, Yuan Z. 2013. Electron competition among nitrogen oxides
674 reduction during methanol-utilizing denitrification in wastewater treatment. Water Res
675 47:3273-81.

676 44. Lycus P, Bøthun KL, Bergaust L, Shapleigh JP, Bakken LR, Frostegård Å. 2017. Phenotypic and
677 genotypic richness of denitrifiers revealed by a novel isolation strategy. ISME J 11:2219–2232.
678 45. Kjelleberg S, Albertson N, Flärdh K, Holmquist L, Jouper-Jaan A, Marouga R, Ostling J, Svenblad
679 B, Weichart D. 1993. How do non-differentiating bacteria adapt to starvation? Antonie Van
680 Leeuwenhoek 63:333-41.
681 46. Gray DA, Dugar G, Gamba P, Strahl H, Jonker MJ, Hamoen LW. 2019. Extreme slow growth as
682 alternative strategy to survive deep starvation in bacteria. Nat Commun 10:890.
683 47. Thorne SH, Williams HD. 1997. Adaptation to nutrient starvation in *Rhizobium*
684 *leguminosarum bv. phaseoli*: analysis of survival, stress resistance, and changes in
685 macromolecular synthesis during entry to and exit from stationary phase. J Bacteriol
686 179:6894-901.
687 48. Lodwig EM, Leonard M, Marroqui S, Wheeler TR, Findlay K, Downie JA, Poole PS. 2005. Role
688 of polyhydroxybutyrate and glycogen as carbon storage compounds in pea and bean
689 bacteroids. Mol Plant Microbe Interact 18:67-74.
690 49. Chen H, Chen CY. 2014. Starvation induces phenotypic diversification and convergent
691 evolution in *Vibrio vulnificus*. PLoS One 9:e88658.
692 50. Zhang X, Nicki G, Kaijalaineni S, Terefework Z, Paulin L, Tighe SW, Graham PH, Lindström K.
693 (1999) Phylogeny and Diversity of *Bradyrhizobium* Strains Isolated from the Root Nodules of
694 Peanut (Arachis hypogaea) in Sichuan, China. Syst Appl Microbiol 22:378-386.
695 51. Schwartz W. 1972. Vincent, J.M. A Manual for the Practical Study of the Root-Nodule Bacteria
696 (IBP Handbuch No. 15 des International Biology Program, London). XI u. 164 S., 10 Abb., 17

Tab., 7 Taf. Oxford-Edinburgh 1970: Blackwell Scientific Publ., 45 s. Z Allg Mikrobiol 12:1521-4028.

52. Mania D, Heylen K, van Spanning RJ, Frostegård Å. 2016. Regulation of nitrogen metabolism in the nitrate-ammonifying soil bacterium *Bacillus vireti* and evidence for its ability to grow using N_2O as electron acceptor. Environ Microbiol 18:2937-50.
53. Cox RD. 1980. Determination of nitrate and nitrite at the parts per billion level by chemiluminescence. Anal Chem 52:332–335.
54. MacArthur PH, Shiva S, Gladwin MT. 2007. Measurement of circulating nitrite and S-nitrosothiols by reductive chemiluminescence. J Chromatogr B Analyt Technol Biomed Life Sci 851:93–105.
55. Conthe M, Lycus P, Arntzen MØ, Ramos da Silva A, Frostegård Å, Bakken LR, Kleerebezm R, van Loosdrecht MCM. 2019. Denitrification as an N_2O sink. Water Res 151:381–387.
56. Cox J, Mann M. 2008. MaxQuant enables high peptide identification rates, individualized p.p.b.-range mass accuracies and proteome-wide protein quantification. Nat Biotechnol 26:1367-72.
57. Ducret A, Quardokus EM, Brun YV. 2016. MicrobeJ, a tool for high throughput bacterial cell detection and quantitative analysis. Nat Microbiol 20:16077.
58. Perez-Riverol Y, Csordas A, Bai J, Bernal-Llinares M, Hewapathirana S, Kundu DJ, et al. 2019. The PRIDE database and related tools and resources in 2019: improving support for quantification data. Nucleic Acids Res 47 (D1): D442-D450 (PubMed ID: 30395289).

Figure legends

FIG 1 Bioassays for assessing the effect of starvation on electron flow to denitrification enzymes. A: Bioassay 1: starvation of cells with a previously expressed denitrification proteome. Cells were raised from stock cultures in fully oxic flasks containing YMB medium. When OD_{600} reached ~0.1, the flasks were made anoxic by He-washing, then supplemented with 1% O_2 in the headspace and 1 mM NO_3^- in the liquid. The cultures were allowed to deplete the O_2 and to initiate denitrification when growing in YMB medium, after which they were centrifuged (10 000 × g at 4 °C for 10 mins) and washed twice in sterile ddH_2O. The pellets from triplicate flasks were pooled and used to inoculate flasks containing either C-free buffer or YMB medium (well-fed control), in both cases supplemented with 1 mM KNO_3 and 0.25 or 0.5 mM KNO_2, and with He and 1 ml N_2O (around 80 µmol N $flask^{-1}$) in headspace. The starving cells, incubated in buffer, had a low respiratory electron flow rate (mol electrons $cell^{-1}$ h^{-1}), initially being 10-18 % that of the well-fed cultures, and then decreasing to reach around 4% after 20 h. Results from experiments using Bioassay 1 are presented in Figs. 2, 3 and 4.

B: Bioassay 2: denitrification induced during starvation. Cells were raised from stock cultures in fully oxic flasks containing YMB medium. When OD_{600} reached ~0.1, the cultures were centrifuged (10 000 × g at 4 °C for 10 mins) and washed twice in sterile ddH_2O. The pellets from triplicate flasks were pooled, after which they were evenly divided and used to inoculate fully oxic flasks containing C-free buffer. These cultures were incubated for 20 h, then centrifuged after which the pellets were pooled and divided evenly before being inoculated into flasks containing C-free buffer provided with 1 mM KNO_3, and with He and 1 ml N_2O (around 80 µmol N $flask^{-1}$) in headspace. The respiration rate (mol electrons $cell^{-1}$ h^{-1}) of the starving cultures was 1-4% compared to that of well-fed cultures. All cultures in Bioassays 1 and 2 were incubated at

741 28°C, and with vigorous stirring (650 rpm). Results from experiments using Bioassay 1 are
742 presented in Figs. 5 and S2.

743

744 **FIG 2** Denitrification kinetics as affected by starvation in cultures with a complete denitrification
745 proteome (Bioassay 1). Cells were allowed to develop a full denitrification proteome under well-
746 fed conditions and were then washed twice in buffer prior to inoculation to flasks with YMB (well-
747 fed control) or buffer (starved), supplemented with 1 mM KNO_3 and 0.25 mM KNO_2, and with He
748 plus 1 ml N_2O (around 80 µmol N) in headspace. A larger inoculum was given to the flasks with
749 buffer (9.9E+08 cells $flask^{-1}$) than to the flasks with YMB (5.0E+09 cells $flask^{-1}$), to secure
750 measurable activity in the starved cells and adequate time resolution of the denitrification
751 kinetics in the well-fed cells. Panels A and B show the denitrification kinetics in well-fed and
752 starved cultures, respectively. The flasks were practically anoxic from the start with an initial O_2
753 concentration in the liquid of <0.52 µM which decreased to approximately 0 µM (insets in A & B).
754 Panels C and D show the cell specific electron flow rate. $V_{e\ total\ den}$ designates the total electron
755 flow to the denitrification reductases and $V_{e\ total\ incl\ O2}$ the total electron flow, including that to
756 denitrification and to O_2. The electron flow rate to the individual reductases is designated as V_{eNap},
757 V_{eNir}, V_{eNor} and V_{eNos}. The rates of NO_3^- reduction (V_{eNap}), which showed that no NO_3^- reduction
758 took place in the starved cultures throughout the entire incubation period, were calculated by N-
759 mass balance for each time increment, as done previously (19, 35). V_{eNir} and V_{eNor} were practically
760 identical and cannot be distinguished from one another in the figure. Inserted panels show V_{eNap}

761 throughout, including negative values which are due to slight errors in determination of N_2 and
762 N_2O (V_{eNap} was calculated by N-mass balance). Bars in all graphs show standard deviation (n=3).

763

764 **FIG 3** Bioassay 1 with single nitrogen oxides**.** Experimental conditions as for Fig. 2, but the starving
765 cells (in buffer) were provided with either NO_3^-, NO_2^- or N_2O in individual flasks (n=3 for each
766 treatment). Panels A-C show the gas kinetics in flasks provided with 1 mM NO_3^- (A), 0.5 mM NO_2^-
767 (B), or 70 µmol N_2O-N added to the headspace (C). Panel D shows the cell-specific electron flow
768 rate (V_e) measured in buffer supplemented with NO_3^-, NO_2^- or N_2O; the O_2 concentration (left y-
769 axis); and V_e as percentage of the rates in well-fed cultures (right y-axis). The number of cells
770 inoculated into the incubation flasks at the start (0 h of incubation in anoxic buffer) was 3.6E+09
771 for all treatments. Bars show standard deviation (n=3).

772

773 **FIG 4** Denitrification in starved cells after addition of TMPD as an external electron donor.
774 Preparation of the cultures followed Bioassay 1 (Fig. 1A), except that 100 µM TMPD and 10 mM
775 ascorbate were injected into the flasks with starving cells 15 min before the first gas sampling.
776 Each flask was inoculated with 5.28E+08 cells (n=4 replicate flasks). The flasks were initially
777 provided with 1 mM initial NO_3^-, 0.25 mM NO_2^- and 1 ml N_2O (around 80 µmol N_2O-N). The initial
778 O_2 concentration was 0.35 µM and decreased to approximately 0 within 5 h (inset in A). Bars show
779 standard deviation (n=4). Panel A: kinetics of NO_2^-, NO, N_2O and N_2 (O_2 in inserted panel). Panel
780 B: Calculated cell specific electron flow rate (V_e, fmol cell^{-1} h^{-1}) to each of the reductases Nap, Nir,
781 Nor, and NosZ, and the total electron flow rate (V_{etotal}). The electron flow to Nir was practically
782 identical to the electron flow to Nor (miniscule amounts of NO), and the two are shown as a single

783 graph ($V_{eNir/Nor}$). Inset plots show V_{eNap} throughout, including negative values which are due to
784 slight errors in determination of N_2 and N_2O (V_{eNap} was calculated by N-mass balance).

785

786 **FIG 5** Bioassay 2: stochasticity of starvation response, response to input of organic C and
787 quantification of denitrification enzymes. Altogether fifteen flasks were prepared following
788 Bioassay 2 (see Fig. 1B). All flasks were anoxic (<0.5 µM at the start of the incubation) and
789 contained 50 ml buffer supplemented with 1 mM KNO_3 and with He plus 1 ml N_2O in the
790 headspace. The NO_2^- concentrations, measured during the first 5 hours after incubation in the
791 buffer, were approximately 0.59±0.20 µM (not shown). The cultures separated into two distinct
792 phenotypes: nine flasks had "slow" respiration (panel A) and 6 flasks had "fast" respiration (panel
793 B). The electron flow to the individual reductases (fmol e^- $cell^{-1}$ h^{-1}) for the flasks with slow and
794 fast respiration are shown in panels C and D, respectively. Cultures with "slow" respiration rate
795 had a total electron flow rate of maximum 0.27 e^- $cell^{-1}$ h^{-1} (C) and cultures with "fast" respiration
796 rate had a total electron flow rate of 1.0-1.8 fmol e- $cell^{-1}$ h^{-1} (D). The inset plot in panel C shows
797 the electron flow to the individual denitrification reductases after the carbon addition. The
798 cultures (entire flasks, 50 ml) were sampled for proteomics analyses at different time points
799 (panels E and F). At timepoints throughout, marked by dashed vertical lines in panels A and B,
800 three flasks were harvested for proteomics analysis (including 0 h). The six flasks with "fast"
801 respiration were harvested for proteomics analysis at 5 and 20 h of incubation in these anoxic
802 buffers (triplicates at each sampling point). Of the nine flasks with "slow" respiration, three were
803 harvested at 10 and three at 20 h. The remaining three "slow" respiration flasks were
804 supplemented with YMB at 24.8 h, at a concentration which made the buffer a half-strength YMB

805 medium, containing 5 g mannitol l^{-1} and 0.25 yeast extract l^{-1}, and then harvested for proteomics
806 at 27 h. The gas measurements and electron flows are averages from the three flasks (n=3) for
807 each phenotype, that were left untouched until the end of the incubation when they were
808 sampled for proteomics. Proteomics analyses were done for triplicate flasks (n=3) at each
809 sampling point. Standard deviations are indicated as bars in all graphs (in several cases not visible
810 due to low variation).
811

Bioassay 1: Denitrification induced before starvation

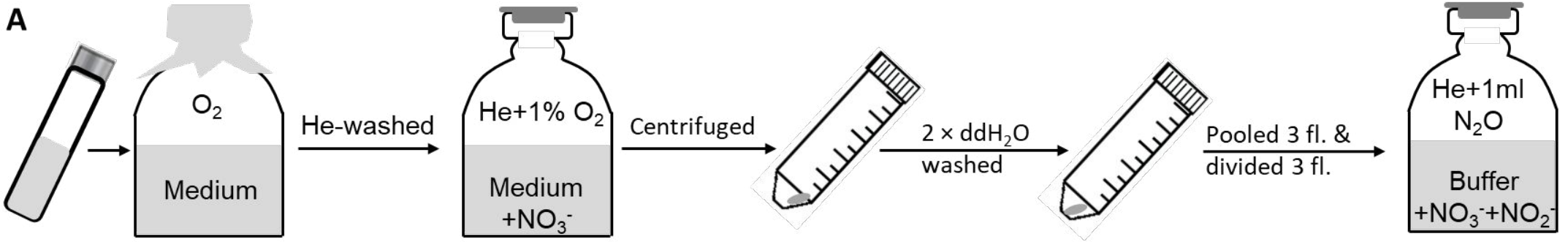

Bioassay 2: Denitrification induced during starvation

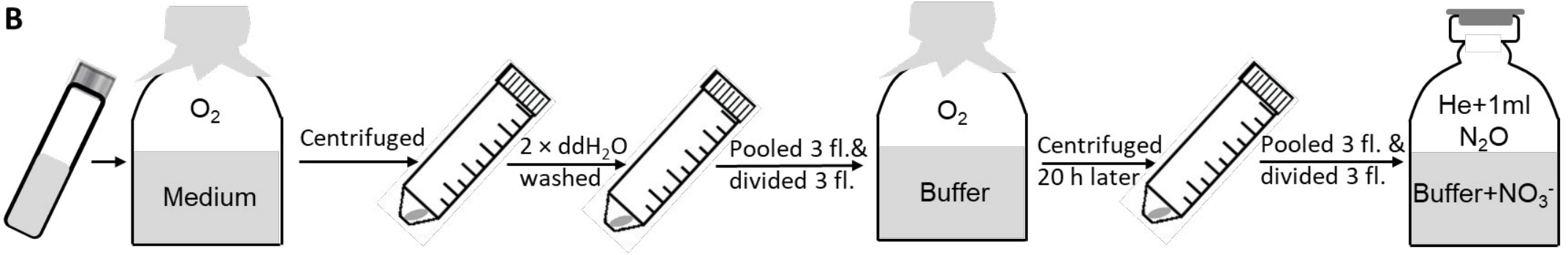

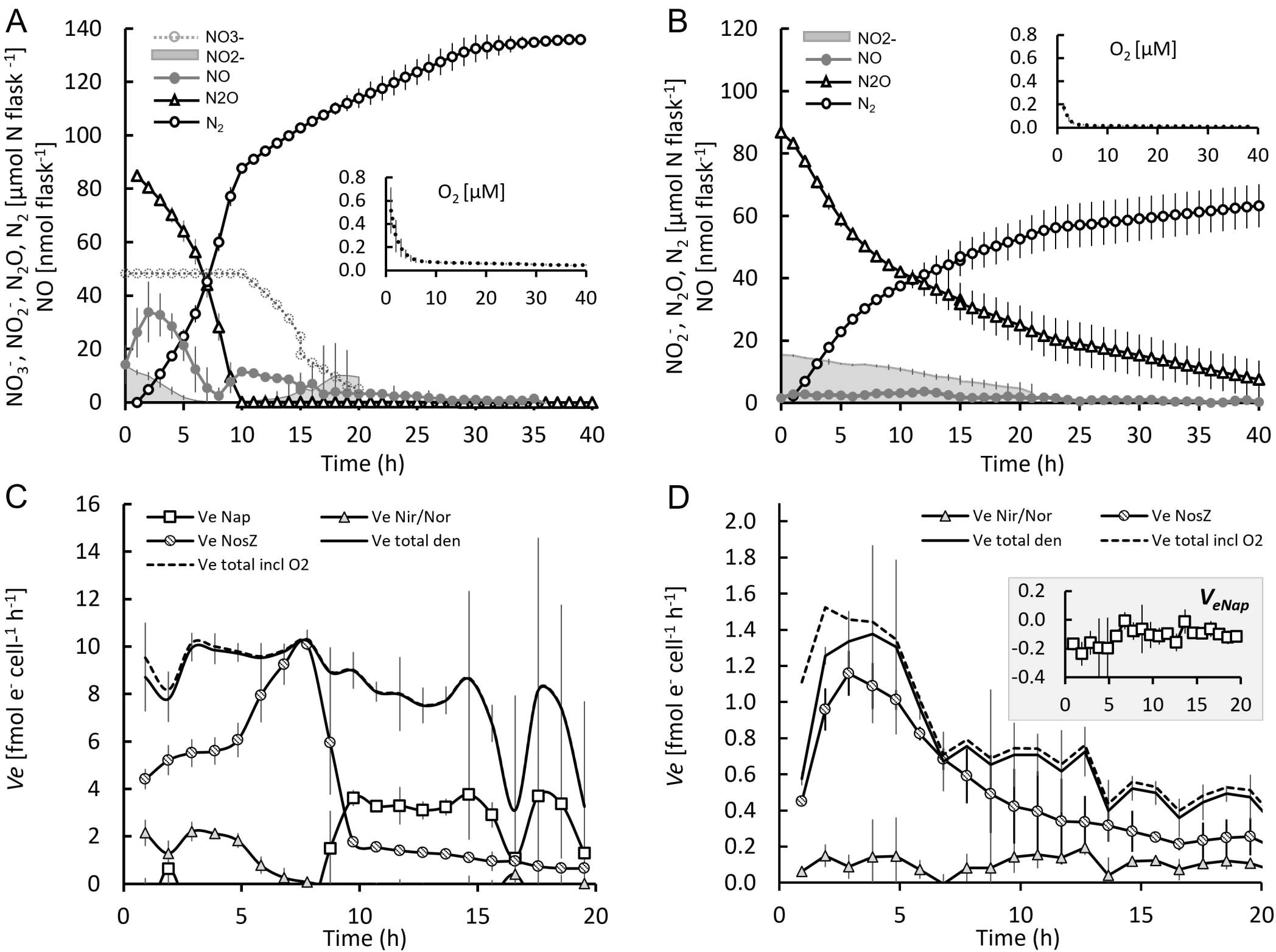
A
NO3-
NO2-
NO
N2O
N2
O2 [µM]
NO3-, NO2-, N2O, N2 [µmol N flask-1]
NO [nmol flask-1]
Time (h)
B
NO2-
NO
N2O
N2
O2 [µM]
NO2-, N2O, N2 [µmol N flask-1]
NO [nmol flask-1]
Time (h)
C
Ve Nap
Ve Nir/Nor
Ve NosZ
Ve total den
Ve total incl O2
Ve [fmol e- cell-1 h-1]
Time (h)
D
Ve Nir/Nor
Ve NosZ
Ve total den
Ve total incl O2
VeNap
Ve [fmol e- cell-1 h-1]
Time (h)

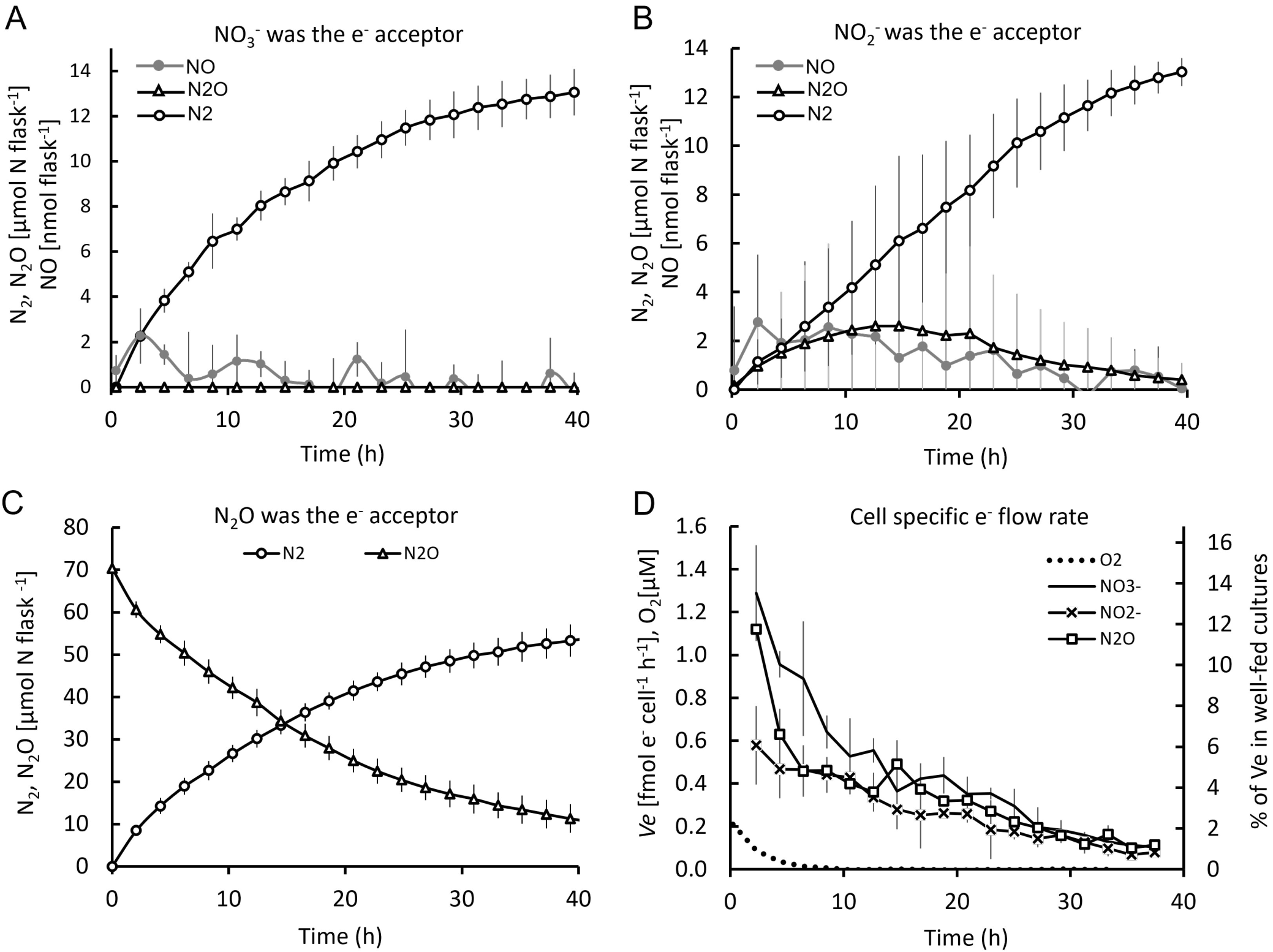
A
NO_3^- was the e- acceptor
NO
N2O
N2
N_2, N_2O [µmol N flask^{-1}]
NO [nmol flask^{-1}]
Time (h)
B
NO_2^- was the e- acceptor
NO
N2O
N2
N_2, N_2O [µmol N flask^{-1}]
NO [nmol flask^{-1}]
Time (h)
C
N_2O was the e- acceptor
N2
N2O
N_2, N_2O [µmol N flask^{-1}]
Time (h)
D
Cell specific e- flow rate
O2
NO3-
NO2-
N2O
Ve [fmol e- cell^{-1} h^{-1}], O_2[µM]
% of Ve in well-fed cultures
Time (h)

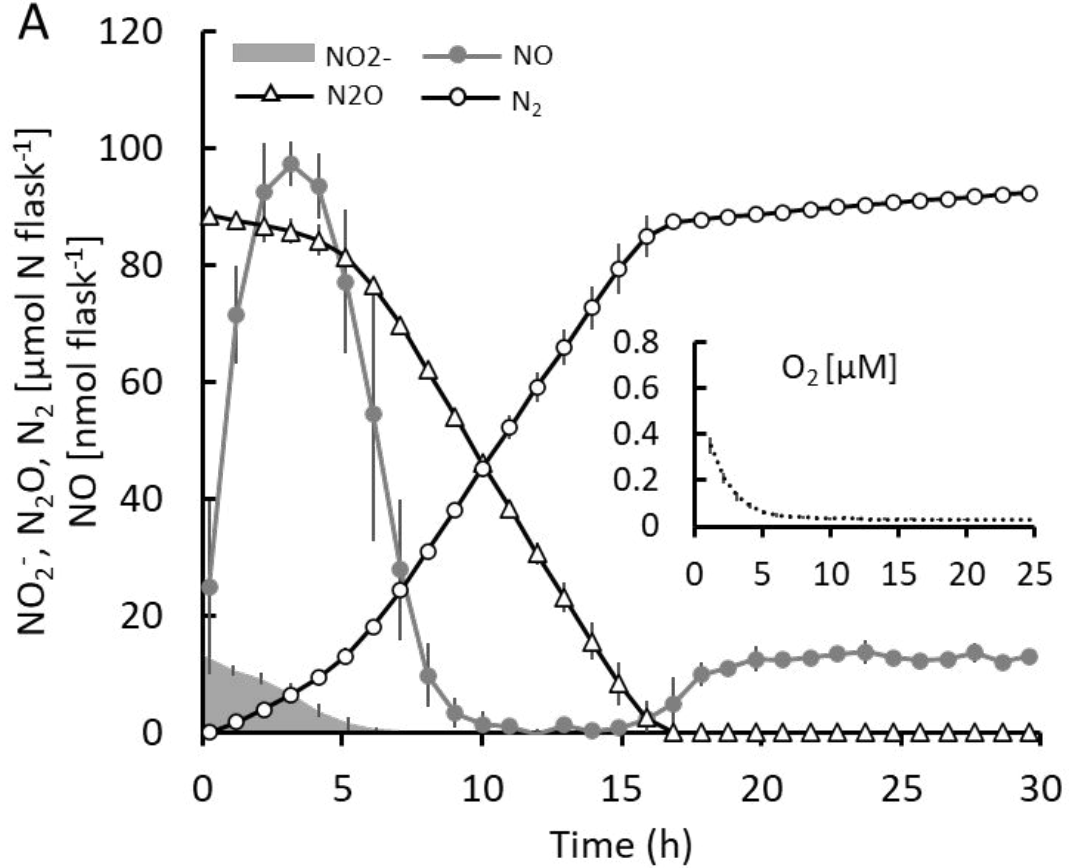
A
NO2-
NO
N2O
N2
O2 [µM]
NO2-, N2O, N2 [µmol N flask-1]
NO [nmol flask-1]
Time (h)

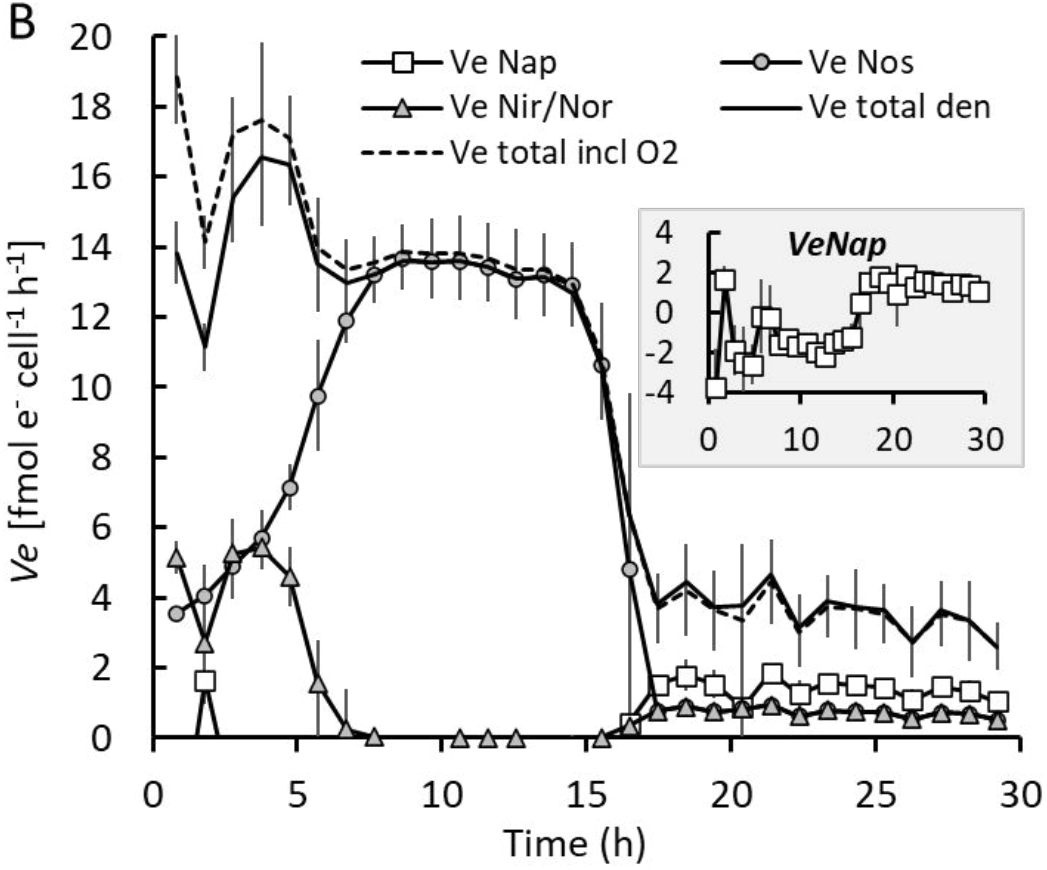
B
Ve Nap
Ve Nos
Ve Nir/Nor
Ve total den
Ve total incl O2
VeNap
Ve [fmol e- cell-1 h-1]
Time (h)

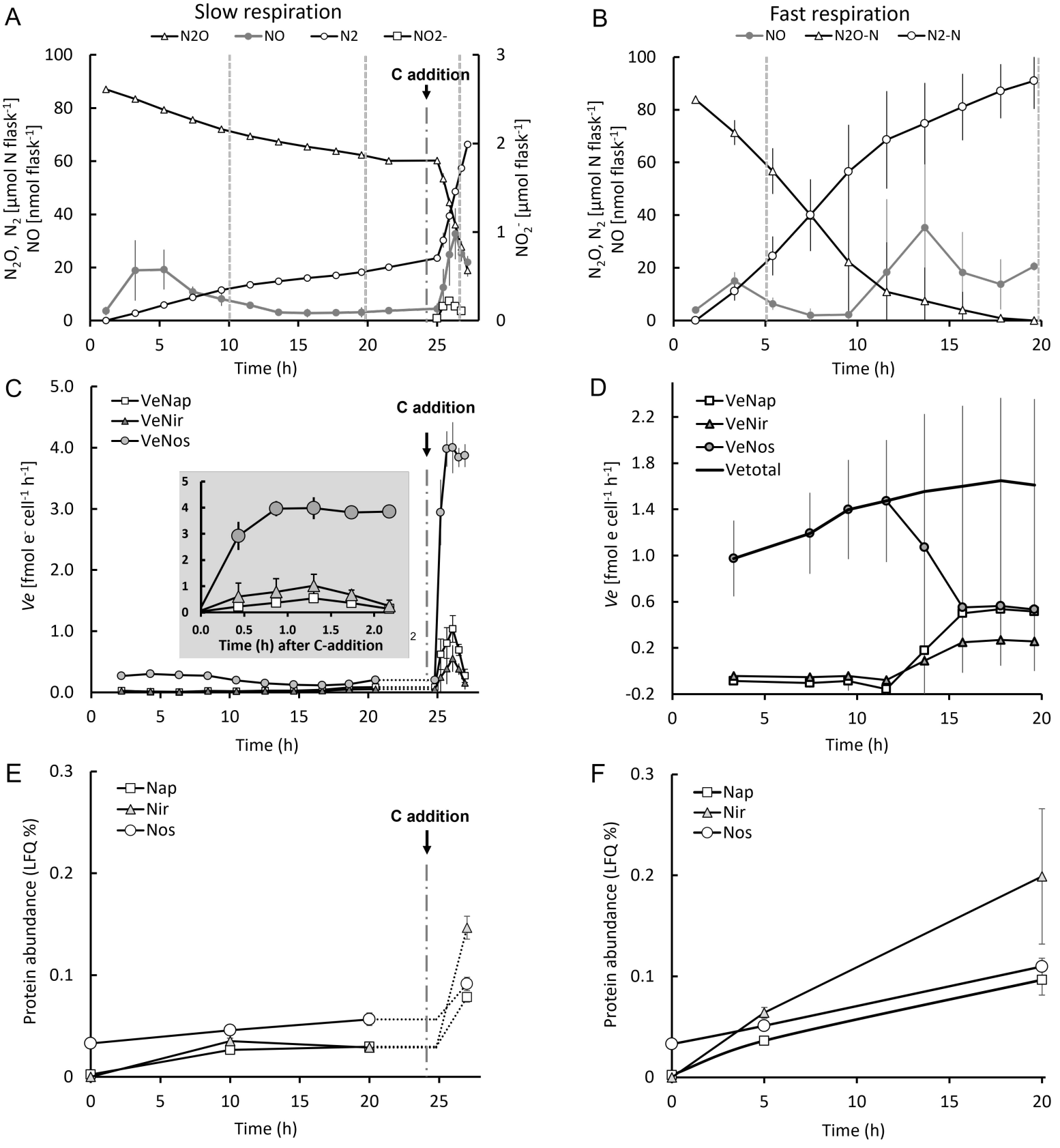
A
Slow respiration
N2O
NO
N2
NO2-
C addition
N2O, N2 [µmol N flask-1]
NO [nmol flask-1]
NO2- [µmol flask-1]
Time (h)
B
Fast respiration
NO
N2O-N
N2-N
N2O, N2 [µmol N flask-1]
NO [nmol flask-1]
Time (h)
C
VeNap
VeNir
VeNos
C addition
Ve [fmol e- cell-1 h-1]
Time (h) after C-addition
Time (h)
D
VeNap
VeNir
VeNos
Vetotal
Ve [fmol e cell-1 h-1]
Time (h)
E
Nap
Nir
Nos
C addition
Protein abundance (LFQ %)
Time (h)
F
Nap
Nir
Nos
Protein abundance (LFQ %)
Time (h)

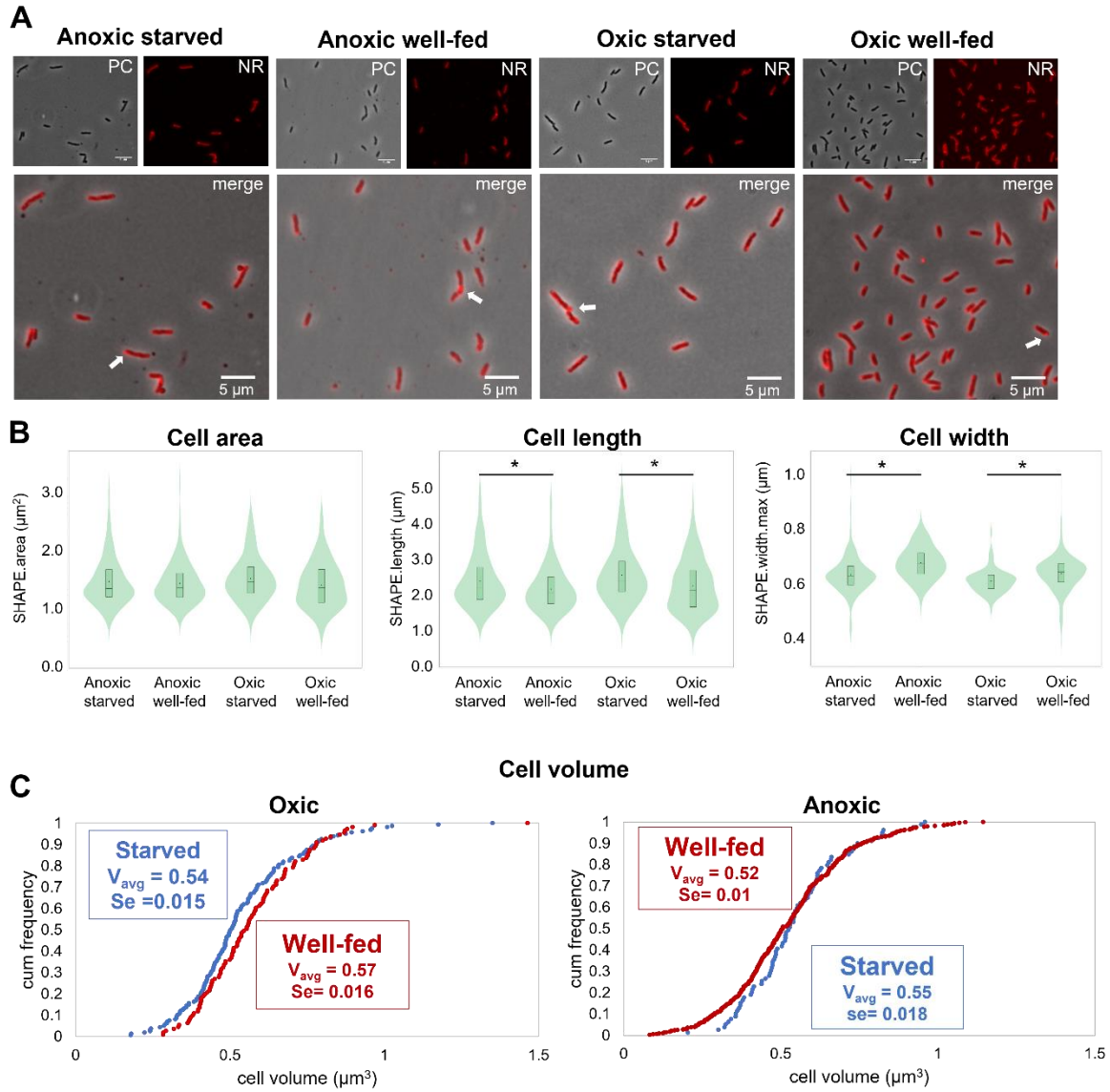

FIG S1 Cell size, morphology and PHA content of *Bradyrhizobium* strain in carbon optimal or carbon starvation condition. To investigate the effect of carbon source and O_2 on the cell morphology, *Bradyrhizobium* strain HAMBI 2125 was raised from stocks in flasks containing YMB medium ("well-fed") or buffer ("starved") with O_2 or N-oxide (NO_3^- or NO_3^- plus N_2O) as electron acceptors. The cultures were incubated at 28 °C with vigorous stirring (600 rpm using a magnetic stirrer) for five days. To secure that the OD_{600} did not exceed 0.1, portions of the culture were regularly inoculated into new flasks. After 5 days, 1 ml volumes of the cultures were taken and fixed in 1 ml of a 1:1 mixture of paraformaldehyde (2% wt/vol) and glutaraldehyde (2.5% vol/vol). The samples were fixed for 1 hour at room temperature and stored over night at 4°C, then observed under microscopy directly or after staining with Nile red. PHA is shown as large Nile Red foci within the cells. White arrows point to examples of such foci. Samples from **oxic well-fed cultures** were taken as control. Other treatments were prepared as follows: **Anoxic well-fed cultures** were prepared following Bioassay 1 (see Fig. 1A, main text). Briefly, flasks containing oxic, well-fed cultures (in YMB medium) with OD_{600} <0.1 were covered by septa and replacing the headspace air with He, 1 mM NO_3^- and 0.7 ml O_2 were added as electron acceptors. Samples were taken after three days of incubation, when the cultures were transitioning from aerobic to anaerobic respiration and thus contained the whole set of denitrifying enzymes. **Oxic starved cultures** were prepared following Bioassay 2 (Fig. 1B in main text), i. e. cultures

incubated oxically in YMB were centrifuged and the cell pellets were washed twice using autoclaved ddH_2O, then added into oxic flasks containing C-free buffer. Samples were taken after 20 h incubation. **Anoxic starved cultures** were prepared following Bioassay 2, i. e. oxically incubated, starved cultures were centrifuged and added into pre-prepared anoxic flasks containing C-free buffer with 1 mM NO_3^- and with 1% N_2O in the headspace. These cultures, which had to synthesize the denitrifying enzymes during carbon starvation, were sampled for microscopic analysis after 3 h of incubation under anoxic, starved conditions. Panel A: Phase contrast (PC), fluorescence (Nile Red, NR) and the merged images of representative cells are shown for all four conditions. PHA is shown as large Nile Red foci within the cells. Panel B: Cell area, cell lengths and cell widths are displayed as violin plots. More than 75 cells were measured for each condition. Asterisks indicate significant differences between samples (Mann-Whitney test, $p < 0.01$). Starvation had a statistically significant effect on both length (increasing) and width (decreasing). Panel C: Distribution of cell volumes (as calculated from width and length of individual cells), and average cell volumes for each treatment as inserts in the panels. Statistically, the effect of starvation on the average cell volume was barely significant for aerobic cells ($p=0.057$), and not for cells grown under anoxic conditions ($p=0.13$).

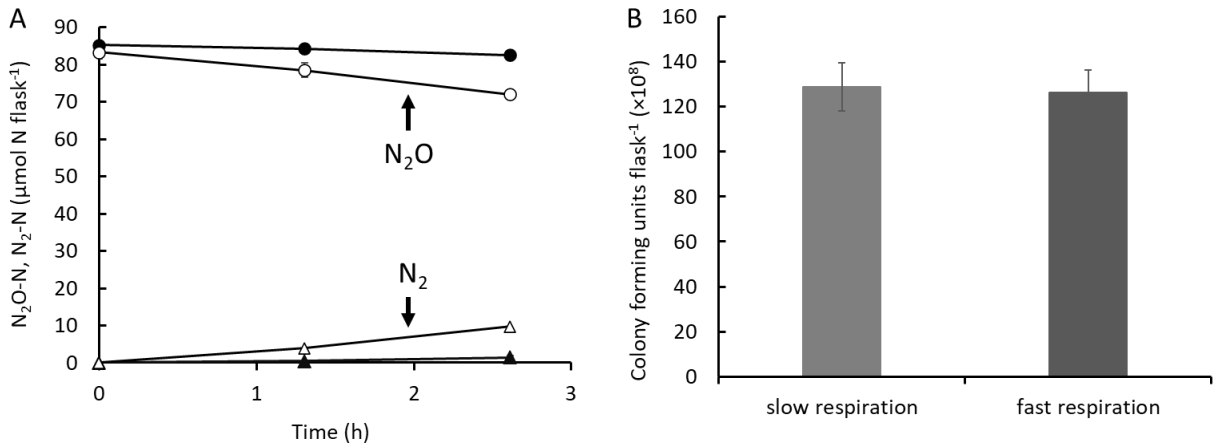

Fig S2 Nitrous oxide reduction and viable counts of cultures with slow *vs* fast respiration rate after exposure to extended starvation (Bioassay 2). Twelve cultures were prepared following Bioasssay 2 (see Fig. 1B in the main text). Triplicate cell pellets were pooled and then divided into three new flasks containing carbon-free buffer with 1 mM NO_3^- and with 1ml N_2O in the headspace. The cultures in four of the flasks showed a "fast" respiration rate (N_2 production rate was 2.51 ±0.86 µmol N flask^{-1}; n=4), while the remaining cultures had a "slow" respiration rate (N_2 production rate was 0.43 ±0.10 µmol N flask^{-1}; n=8). Three flasks of each phenotype were chosen for viable counts to determine if cell lysis may have occurred in the cultures with "fast" respiration. **A.** Gas measurements for three flasks of each phenotype ("slow" or "fast" respiration) from which samples for viable counts were taken. N_2O reduction (circles) and N_2 production (triangles) in "fast" (open symbols) and "slow" cultures (filled symbols). Bars represent standard deviation (n=3) but are in most cases too small to be visible. **B.** Viable counts (colony forming units; CFU). Samples (1 ml) were taken from each flask after 3.1 h of anoxic incubation in C-free buffer (last step of the assay). The OD_{600} at this time point was not significantly different between the cultures with fast vs slow respiration rate ($P > 0.3$). Diluted samples were streaked on YMA (yeast mannitol agar) plates. No difference in CFU flask^{-1} was found between the cultures with fast respiration rate and slow respiration rate ($P=0.4$). The bars represent standard deviation (n=3).

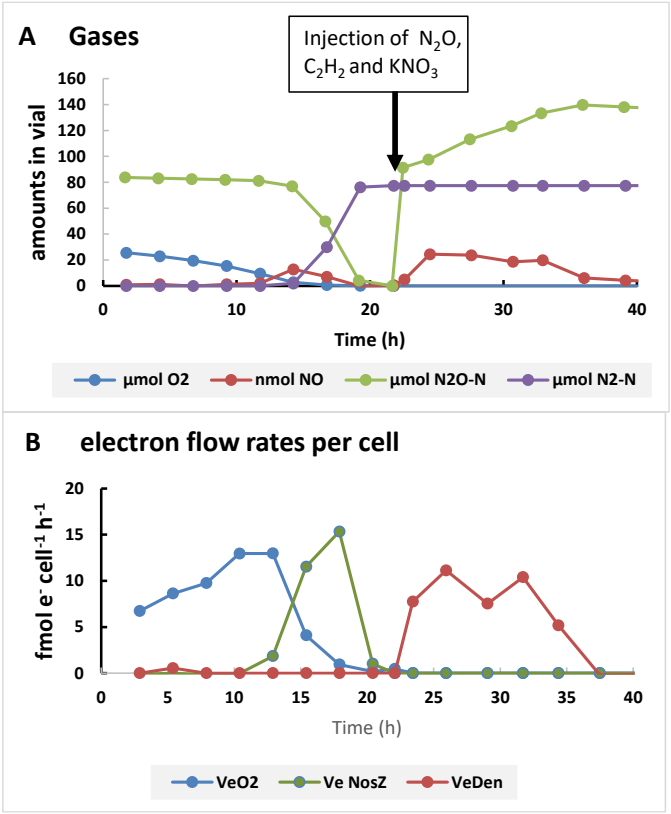

Fig S3 Does N_2O hamper NapA directly? An alternative explanation to the low/zero NapA-activity in cells provided with N_2O could be that N_2O inhibits NapA directly, rather than via competition for electrons. This was effectively tested in the experiments by Mania et al (Environ Microbiol 2020, 22:17–31), who exposed a closely related *Bradyrhizobium* strain (AC87j1) to 10 vol % acetylene (inhibiting NosZ) and 10 vol% N_2O. The gas kinetics during these incubations effectively proves that N_2O has no direct inhibitory effect on NapA. The panels show the result for a single vial inoculated with $4.8*10^8$ cells, provided with 8 vol% O_2 and 10 vol% N_2O. This stirred batch culture (50 mL liquid medium in 120 mL gas tight vials, incubated at 28 °C) was allowed to deplete the oxygen and N_2O, and then provided with KNO_3 (0.5 mL 100 mM KNO_3), and 10 vol% of both N_2O and acetylene (all by injection through the septum). Based on the measured gas kinetics, shown in **Panel A**, the electron flow rates per cell for each time increment were calculated, based on gas transformation rates and cell density as calculated from the cumulated electron flow to the different electron acceptors. **Panel B** shows the electron flow rates (fmol e^- $cell^{-1}$ h^{-1}): V_{eO2} is the electron flow rate to O_2, V_{eNosZ} is the electron flow rate to N_2O, an V_{eDen} is the sum of the electron flow rates to NO_3^-, NO_2^- and NO. After injection of acetylene, N_2O and NO_3^- (indicted in Panel A), V_{eDen} fluctuated between 5 and 10 fmol e^- cell h^{-1} until depletion of NO_3^-. This means that the NO_3^- reduction rate fluctuated between 1.25 and 2.5 fmol NO_3^- $cell^{-1}$ h^{-1}, which is the same range as observed in vials without acetylene and N_2O (not shown). This shows that N_2O has no direct inhibitory effect on NapA.

Practically identical results were found in the replicate vial.

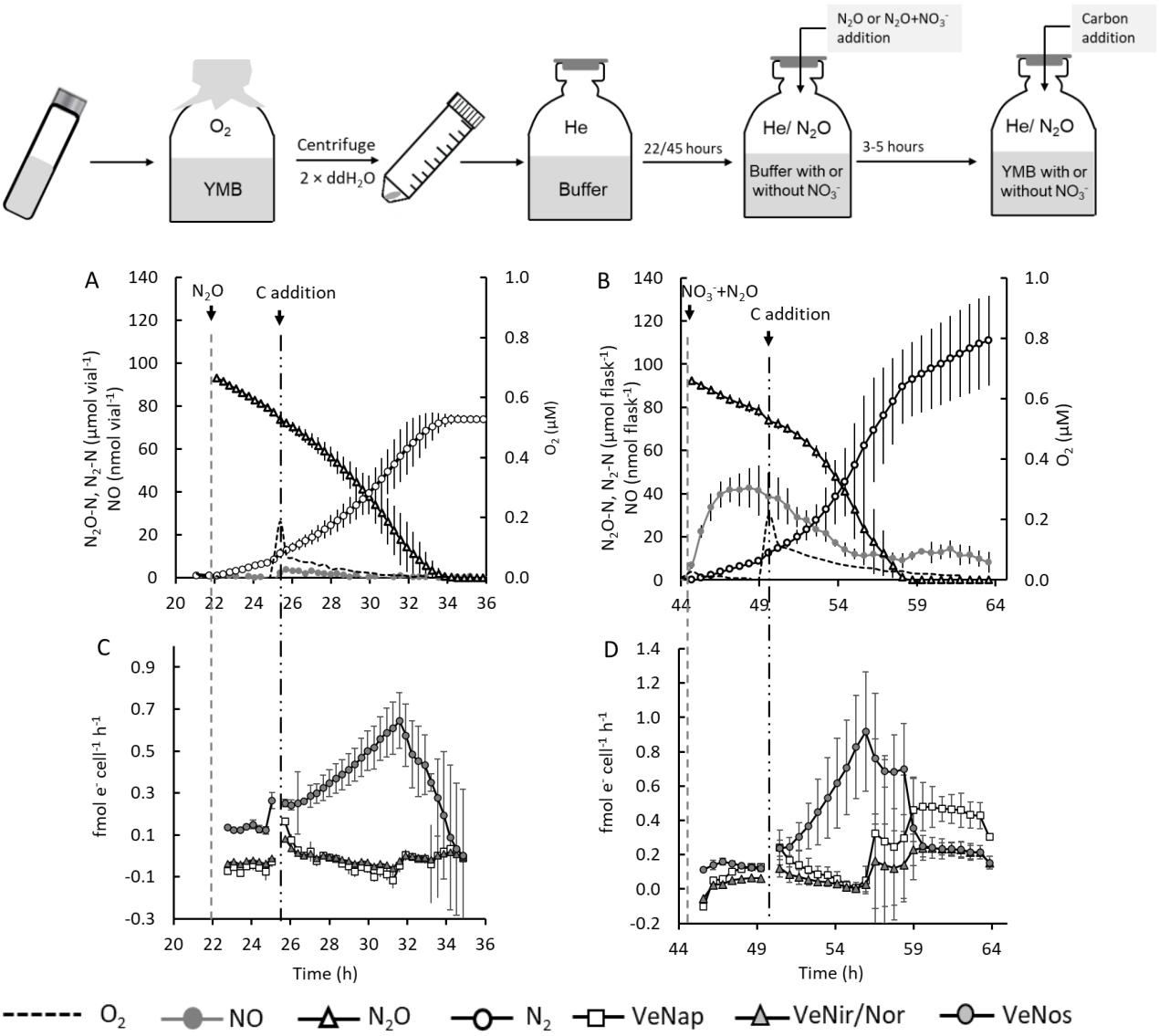

FIG S4 Denitrification kinetics of starved cultures of *Bradyrhizobium* strain HAMBI 2125 and response to carbon addition. Gas kinetics and corresponding electron flow rates of starved cultures provided with N_2O (**Panels A and C**) or N_2O and NO_3^- (**Panels B and D**) as electron acceptor. The bioassay protocol for preparations of the cultures, depicted above the figure panels, was similar to Bioassay 2 (Fig. 1B, main text) where the organisms had to synthesize the denitrification proteome in the absence of a carbon source. The cultures were raised from stocks in YMB medium. After five days the cultures were centrifuged and washed twice using autoclaved ddH_2O, after which the pellets were added into pre-prepared flasks containing C-free buffer and He in headspace. No pooling of pellets took place (as opposed to Bioassay 2). The flasks (triplicate samples for each treatment) contained 9.1-10.0E+9 cells (N_2O treated cultures) or 1.50-1.52 E+10 cells (flasks with N_2O + NO_3^-). The O_2 concentration was < 0.2 µM in the anoxic incubation steps having He or He and N_2O in headspace. After three to five hours of incubation in buffer with N-oxides, each flask received a portion of YMB (marked with dashed-dotted line), resulting in a full-strength medium (10 g/l mannitol plus 0.5 g/l yeast extract). The negative electron flow to denitrification reductases in some sampling points may be due to minor errors in calibration of N-gas measurements, as explained in detail in the main text. Bars in all graphs show standard deviation (n=3).